Electronic Supplementary Information

Naphthalenediimide-carbonylpyridiniums: Stable Six Electron Acceptors for Organic Cathodes

*Qiting Lin, Heyang Li, Ling Chen, Xiaoming He**

*To whom correspondence should be addressed

Key Laboratory of Applied Surface and Colloid Chemistry (Ministry of Education), School of Chemistry and Chemical Engineering, Shaanxi Normal University, Xi'an 710119, P.R. China

*Corresponding Author Email: xmhe@snnu.edu.cn

EXPERIMENTAL SECTION

Materials and Methods. Polyvinylidene fluoride (PVDF) and 1-methyl-2-pyrrolidinone (NMP) were purchased from Shenzhen Kejing Zhida Technology Co., Ltd. $LiClO_4$, tetraglyme (G4), CR2032 battery case, and separator (polypropylene, Celgard 2400) were purchased from DoDoChem. All other chemical reagents were purchased from commercial sources (Aldrich, Alfa Aesar, Strem and Adamas) and were, unless otherwise noted, used without further purification.

^{1}H NMR and ^{13}C NMR spectra were recorded on 400 MHz and 600 MHz BRUKER spectrometers. Chemical shifts were referenced to residual non-deuterated solvent peaks. Mass spectrometry data were collected on a Bruker maxis UHR-TOF mass spectrometer in ESI positive mode. PXRD patterns were recorded on a Bruker D8 Advance instrument with Cu Kα X-ray radiation (λ=1.5406 Å). TGA was conducted under a nitrogen atmosphere on a TA Q600 instrument with a heating rate of 10 °C min. Ultraviolet–visible (UV-vis) absorption spectra were recorded on a Cary 3500 spectrometer. Scanning electron microscope (SEM) images were recorded using a Hitachi SU8220 system. Cyclic voltammetry (CV) was performed on a Shanghai Chenhua CHI760E instrument, with a polished glassy carbon electrode as the working electrode, a Pt-wire as counter electrode, and Ag/AgCl as a reference electrode, using ferrocene/ferrocenium (Fc/Fc^+) as internal standard. CV experiments for small molecules were performed in DMF solution with tetrabutylammonium hexafluorophosphate (0.05 M) as supporting electrolyte. Theoretical calculations have been carried out at the B3LYP/6-31G(d,p) level by using the GAUSSIAN 09 suite of programs.

Synthesis of 2,6-dibromonaphtalene-1,4,5,8-tetracarboxylicdianhydride (S0). This was synthesized according to previously reported protocol.[S1] In 250 mL single-necked RB flask, 10.72 g (40 mmol, 1 eq) of naphthalene-1,4,5,8-tetracarboxylicdianhydride was stirred in concentrated sulfuric acid (100 mL) at room temperature, the mixture was stirred at room temperature for 5 min to obtain a solution. Then, 17.16 g (60 mmol, 1.5 eq) of 1,3-dibromo-5,5-dimethylhydantoin (DBH) was added in four portions over a period of 1 h at room temperature. The reaction mixture was heated to 50ºC for 24 h. After cooling to room temperature, the resulting brown solution was poured into crushed ice to precipitate the solid. The precipitated solid was filtered, washed with water then with methanol, and finally dried under vacuum to afford grayish solid that will be used without further purification. Yield: 14.0 g, 80 %. ^{1}H NMR (600 MHz, DMSO-d_6): δ/ppm = 8.80 (s, 2H; Ar*H*). Characterization data

matches literature values.

Synthesis of 2,6-dibromonaphthalene-1,4,5,8-tetracarboxylic-N,N'-bis(octyl) diimide (S1). This was synthesized according to previously reported protocol.[S2] A mixture of 2,6-dibromo-1,4,5,8-naphthalenetetracarboxylic dianhydride (2.56 g, 6 mmol), 1-octylamine (3.10 g, 24 mmol) and acetic acid (100 mL) was stirred at 100 ºC for 5 hours under nitrogen atmosphere. After cooling to room temperature, the precipitate was collected by filtration and washed with water and methanol. Recrystallization from chloroform furnished 2,6- dibromonaphthalene-1,4,5,8-tetracarboxylic-N,N'-bis(octyl) diimide as orange solid (1.8 g, 45 %). ^{1}H NMR (600 MHz, $CDCl_3$): δ/ppm = 9.00 (s, 2H; Ar*H*), 4.19 (t, *J* = 7.2 Hz, 4H; NCH_2), 1.74 (m, 4H; CH_2), 1.23-1.45 (m, 20H; CH_2), 0.88 (t, *J* = 6.6 Hz, 6H; CH_3). Characterization data matches literature values.

Synthesis of 2,6-dibromonaphthalene-1,4,5,8-tetracarboxylic-N,N'-bis(butyl) diimide (S2). The procedure was similar to that used to prepare 2,6-dibromonaphthalene-1,4,5,8-tetracarboxylic-N,N'-bis(octyl) diimide, except 1-butylamine (1.8 g, 24 mmol) was used in place of 1-octylamine. The desired product was isolated as organge solids (74%). ^{1}H NMR (600 MHz, $CDCl_3$): δ/ppm = 9.00 (s, 2H; Ar*H*), 4.20 (t, *J* = 7.2 Hz, 4H; NCH_2), 1.73 (m, 4H; CH_2), 1.46 (m, 4H; CH_2), 1.00 (t, *J* = 7.2 Hz, 6H; CH_3).

Synthesis of ($A1^{2+}$)Br_2. A mixture of 2,6-dibromonaphthalene-1,4,5,8-tetracarboxylic-N,N'-bis(octyl) diimide (324 mg, 0.5 mmol), 4-benzoylpyridine (366 mg, 2.0 mmol) in dry dioxane (10 mL) was stirred at 100 ºC for 48 hours under nitrogen atmosphere. After cooling down to room temperature, the reaction mixture was diluted with diethyl ether (40 mL). The precipitate was filtered, washed with dichloromethane (10 mL) and acetone (10 mL), and dried under vacuum at 50 ºC for 4 h. The desired product was isolated as yellow solids (415 mg, 82 %). ^{1}H NMR (600 MHz, DMSO-d_6): δ/ppm = 9.64 (d, *J* = 6.0 Hz, 4H; C_5H_4N), 9.27 (s, 2H; Ar*H* of NDI), 8.73 (d, *J* = 6.0 Hz, 4H; C_5H_4N), 7.97 (d, *J* = 7.8 Hz, 4H; C_6H_5), 7.90 (t, *J* = 7.8 Hz, 2H; C_6H_5), 7.74 (t, *J* = 7.8 Hz, 4H; C_6H_5), 3.98 (br, 4H; NCH_2), 1.60 (m, 4H; CH_2), 1.40-1.20 (m, 20H; CH_2), 0.85 (m, 6H; CH_3). ^{13}C NMR (150 MHz, DMSO-d_6): δ = 192.57, 161.24, 160.82, 154.88, 147.43, 142.98, 135.66, 134.62, 131.71, 130.84, 129.73, 128.05, 127.76, 127.06, 122.09, 41.10, 31.66, 29.06, 28.99, 27.57, 26.85, 22.52, 14.39. HRMS: m/z calculated for $C_{54}H_{54}N_4O_6^{2+}$ $[M-2Br]^{2+}$ 427.2016, found 427.2018.

Synthesis of ($B1^{2+}$)Br_2. The procedure was similar to that used to prepare **A1**, except 4-acetylpyridine (242 mg, 2.00 mmol) was used in place of 4-benzoylpyridine. The desired product was isolated as yellow solids (392 mg, 88 %). ^{1}H NMR (600 MHz, DMSO-d_6): δ/ppm = 9.68 (br, 4H; C_5H_4N), 9.20 (s, 2H; Ar*H* of NDI), 8.82 (br, 4H; C_5H_4N), 3.92 (br, 4H; NCH_2), 2.91 (s, 6H; CH_3), 1.56 (br, 4H; CH_2), 1.35-1.15 (br, 20H; CH_2), 0.85 (m, 6H; CH_3). No well-resolved ^{13}C NMR spectrum could be obtained due to its limited solubility. HRMS: m/z calculated for $C_{44}H_{50}N_4O_6^{2+}$ $[M-2Br]^{2+}$ 365.1860, found 365.1864.

Synthesis of ($C1^{2+}$)Br_2. The procedure was similar to that used to prepare **A1**, except ethyl isonicotinate (302 mg, 2.00 mmol) was used in place of 4-benzoylpyridine. The desired product was isolated as yellow solids (427 mg, 90 %). ^{1}H NMR (600 MHz, DMSO-d_6): δ/ppm = 9.66 (br, 4H; C_5H_4N), 9.21 (s, 2H; Ar*H* of NDI), 8.85 (br, 4H; C_5H_4N), 4.56 (m, 4H; OCH_2), 3.92 (br, 4H; NCH_2), 1.56 (br, 4H; CH_2), 1.46 (m, 6H; OCH_2CH_3), 1.35-1.15 (m, 20H; CH_2), 0.85 (t, J = 6.6 Hz, 6H; CH_3). ^{13}C NMR (150 MHz, DMSO-d_6): δ (ppm) = 162.58, 161.15, 160.78, 148.12, 146.61, 142.81, 131.61, 127.92, 127.71, 127.45, 122.11, 63.81, 41.08, 31.64, 29.05, 28.96, 27.52, 26.84, 22.50, 14.41, 14.38. HRMS: m/z calculated for $C_{46}H_{54}N_4O_8^{2+}$ $[M-2Br]^{2+}$ 395.1965, found 395.1969.

Synthesis of ($A2^{2+}$)Br_2. The procedure was similar to that used to prepare **A1**, except **S2** (268 mg, 0.5 mmol) and DMF (10 mL) was used in place of **S1** and dioxane. The desired product was isolated as yellow solids (334 mg, 74 %). ^{1}H NMR (600 MHz, DMSO-d_6): δ/ppm = 9.66 (d, J = 6.0 Hz, 4H; pyridine), 9.27 (s, 2H; Ar*H* of NDI), 8.72 (d, 4H, J = 6.6 Hz; pyridine), 7.96 (d, 4H, J = 7.8 Hz; C_6H_5), 7.89 (t, 2H, J = 7.2 Hz; C_6H_5), 7.74 (t, 4H, J = 7.8 Hz; C_6H_5), 4.00 (t, 4H, J = 7.8 Hz; NCH_2), 1.60 (m, 4H; NCH_2CH_2), 1.35 (m, 4H; CH_2CH_3), 0.91 (t, J=7.2 Hz; 6H; CH_2CH_3). ^{13}C NMR (150 MHz, DMSO-d_6): δ = 192.61, 161.27, 160.84, 154.87, 147.42, 142.97, 135.67, 134.63, 131.72, 130.85, 129.73, 128.05, 127.77, 127.07, 122.09, 40.89, 29.75, 20.17, 14.12. HRMS: m/z calculated for $C_{46}H_{38}N_4O_6^{2+}$ $[M-2Br]^{2+}$ 371.1390, found 371.1387.

Synthesis of ($B2^{2+}$)Br_2. The procedure was similar to that used to prepare **B1**, except **S2** (268 mg, 0.5 mmol) was used in place of **S1**. The desired product was isolated as yellow solids (310 mg, 80 %). ^{1}H NMR (600 MHz, DMSO-d_6): δ/ppm = 9.66 (br, 4H; pyridine), 9.18 (s, 2H; Ar*H* of NDI), 8.81 (s, 4H; pyridine), 3.93 (s, 4H; NCH_2), 2.89 (s, 6H; $COCH_3$), 1.54 (m, 4H; NCH_2CH_2), 1.31 (m, 4H; CH_2CH_3) 0.87 (t, 6H, J=7.2 Hz; CH_2CH_3). No well-resolved ^{13}C NMR spectrum could be obtained

due to its limited solubility. HRMS: m/z calculated for $C_{36}H_{34}N_4O_6^{2+}$ $[M\text{-}2Br]^{2+}$ 309.1234, found 309.1230.

Synthesis of ($C2^{2+}$)Br_2. The procedure was similar to that used to prepare **C1**, except **S2** (268 mg, 0.5 mmol) was used in place of **S1**. The desired product was isolated as yellow solids (343 mg, 82 %). ^{1}H NMR (600 MHz, DMSO-d_6): δ/ppm = 9.64 (d, 4H, J = 6.6 Hz; pyridine), 9.21 (s, 2H; Ar*H* of NDI), 8.85 (d, 4H, J = 6.6 Hz; pyridine), 4.56 (q, 4H, J = 6.6 Hz; OCH_2), 3.94 (t, 4H, J = 7.2 Hz; NCH_2), 1.55 (m, 4H; NCH_2CH_2), 1.46 (t, 6H, J = 7.2 Hz; OCH_2CH_3), 1.32 (m, 4H; CH_2CH_3), 0.89 (t, 6H, J=7.2 Hz; CH_2CH_3). ^{13}C NMR (150 MHz, DMSO-d_6): δ (ppm) = 162.11, 160.68, 160.31, 147.64, 146.11, 142.28, 131.13, 127.43, 127.25, 126.96, 121.64, 63.30, 39.52, 29.19, 19.69, 13.93, 13.63. No well-resolved ^{13}C NMR spectrum could be obtained due to its limited solubility. m/z HRMS: calculated for $C_{38}H_{38}N_4O_8^{2+}$ $[M\text{-}2Br]^{2+}$ 340.1236, found 340.1231.

Battery Fabrication and Testing. The working electrodes were prepared by casting slurries containing 50 wt % active materials, 40 wt % conductive carbon black (ECP-600JD) and 10 wt % poly(vinylidene fluoride) (PVDF) binder on carbon paper with a diameter of 12 mm. The average loading of active materials in each pallet was about 0.4-0.6 mg cm^{-2}. The fully prepared electrodes were then dried at 80 °C overnight in a vacuum oven in order to remove any residual solvent. The CR2032-type coin cells were assembled with the cathode pellet, a Celgard 2400 membrane separator, a lithium foil anode and 2.0 mol/L $LiClO_4$/tetraglyme (G4) as electrolyte solution. All the cells were assembled in an argon-filled glove box (< 0.1 ppm of oxygen and < 0.01 ppm of water). The batteries were stood for 12 h before testing. The galvanostatic charge/discharge tests at different current densities are performed on LAND CT2001A battery system at 30°C within the voltage window of 1.2-3.8V. Cyclic voltammetry and electrochemical impedance spectroscopy were performed with the coin cells using an electrochemical workstation (CHI760E). Electrochemical impedance spectroscopy was performed at a frequency range of 100 kHz to 0.1 Hz.

Calculations of the Electrochemical Metrics

Theoretical capacity (C_{theor}, mAh g^{-1}) was calculated according to the equation (1):

$$C_{theor} = \frac{nF}{3.6 \times M} \qquad (1)$$

where n is the number of electrons transferred per molecules, F is the Faraday's constant (96484 C mol^{-1}), M is molecular weight of the molecules (for small molecules) or repeating unit (for polymers).

The b-value and capacitive contribution at a particular potential were determined as follows:

The relationship between scan rate (υ, mV s^{-1}) in a CV and the corresponding cathodic or anodic peak current (i_p, A g^{-1}) is shown in equation (2).[S3] The b-value was the slope of the log(v)-log(i_p) plots according to equation (3).

$$i_p = av^b \qquad (2)$$

$$\log(i_p) = \log(a) + b\log(v) \qquad (3)$$

where a and b are adjustable parameters.

Moreover, the relationship between the current at a particular potential (i(V), A g^{-1}) and the scan rate (υ, mV s^{-1}) is shown in equation (4).[S4] Solving for the values of k_1 and k_2 at each potential, we can obtain the percentage of capacitive contribution the total current (k_2v/i(V)).

$$i(V) = k_1v^{1/2} + k_2v \qquad (4)$$

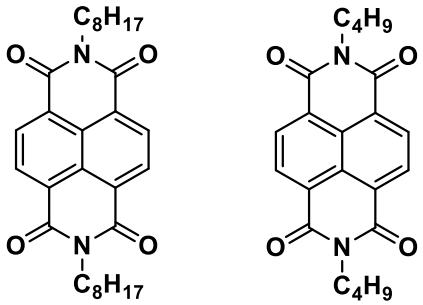

NDI-C8 NDI-C4

Scheme S1. Structure of **NDI-C8** and **NDI-C4** used in this work as prototype compounds.

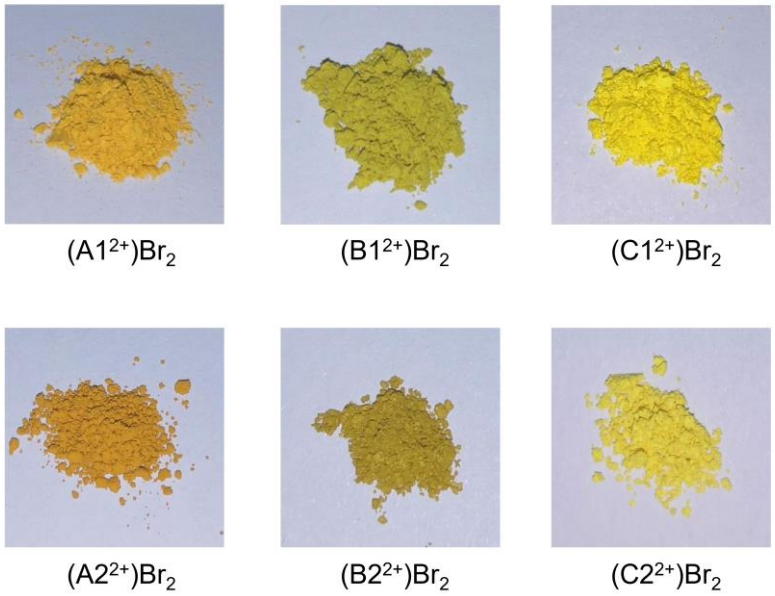

Figure S1. Pictures of the six compounds.

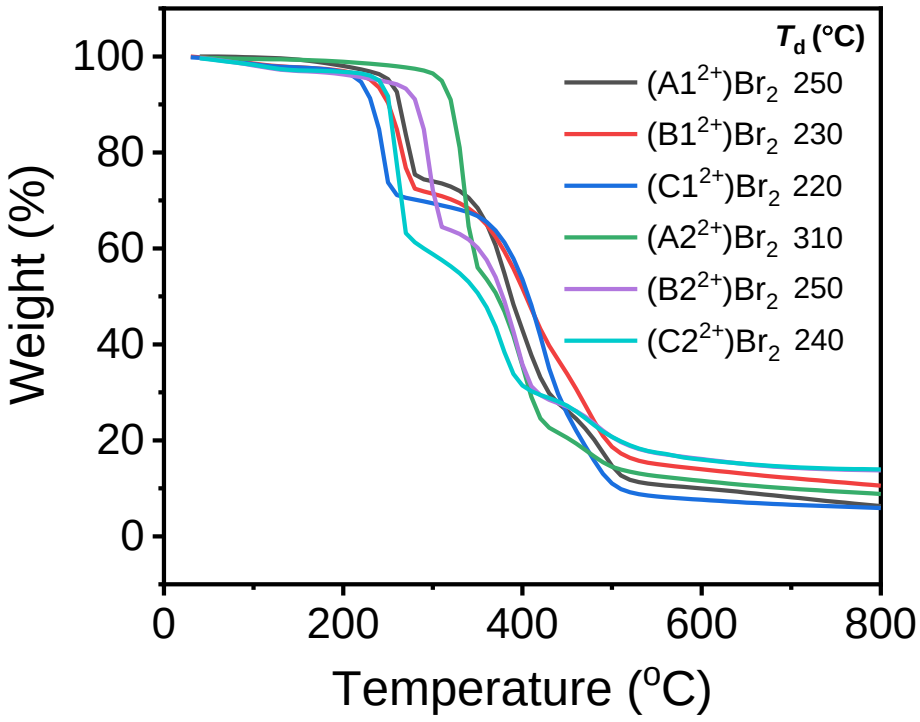

Figure S2. TGA of six NDI-carbonylpyridinium conjugates.

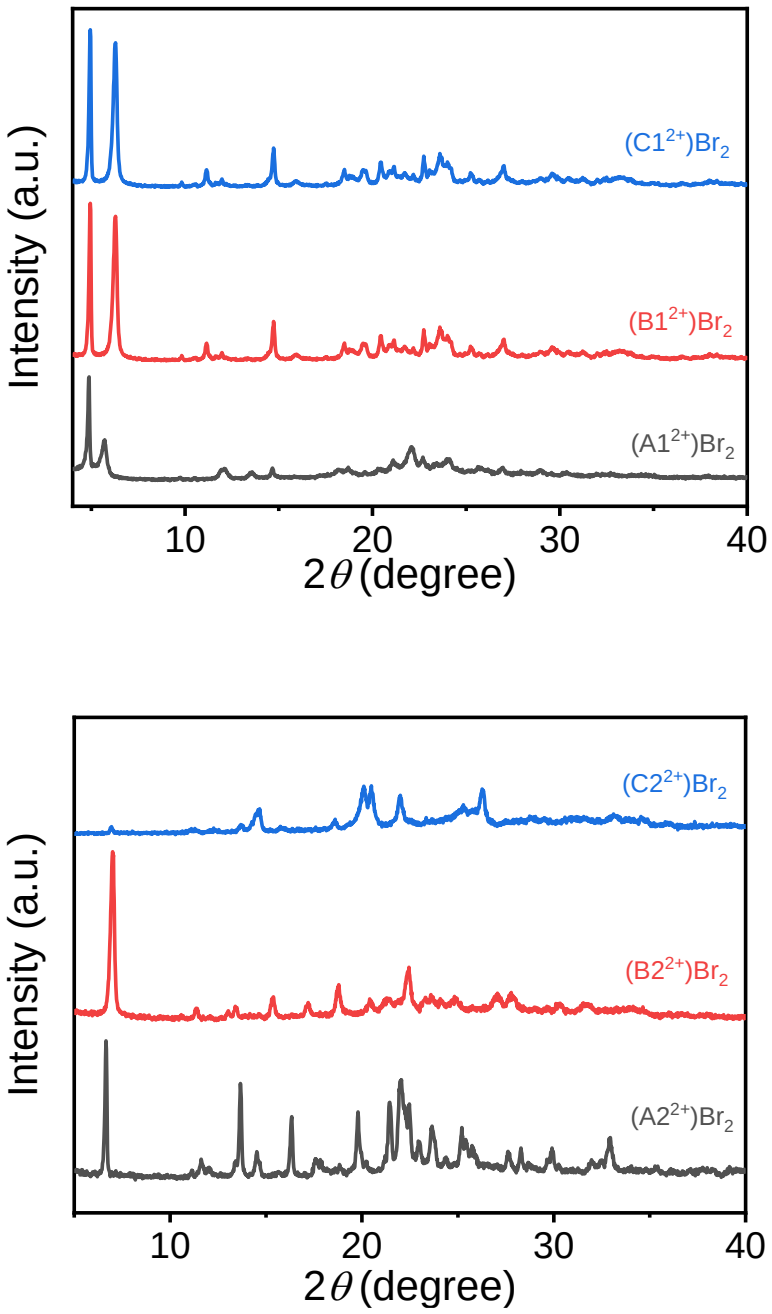

Figure S3. XRD of six NDI-carbonylpyridinium conjugates.

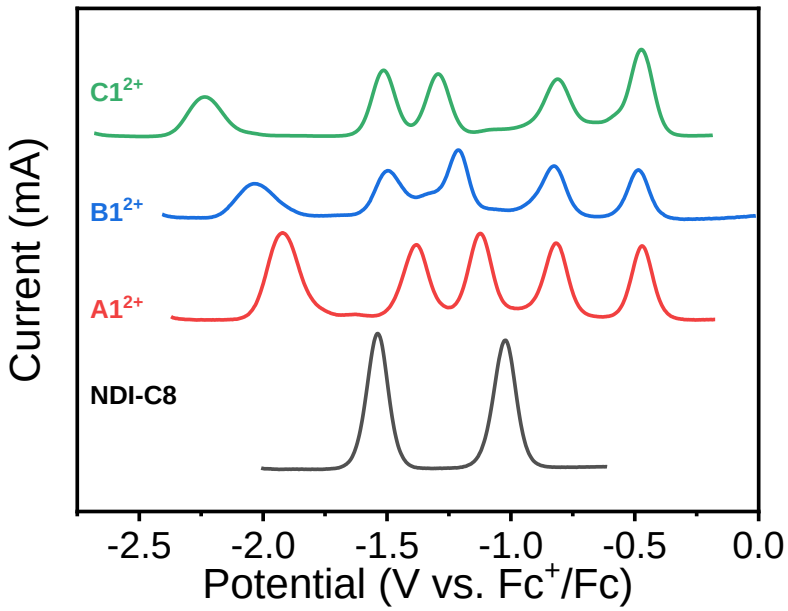

Figure S4. DPVs of **A1**$^{2+}$, **B1**$^{2+}$, **C1**$^{2+}$ and **NDI-C8** in DMF solution (c = 1 mM), with 0.1 M $TBAPF_6$ as the electrolyte. DPV parameters: Increase E = 4 mV, amplitude = 50 mV, pulse width = 60.0 ms, sampling width = 20.0 ms, pulse period = 500.0 ms. The structure of **NDI-C8** is shown in Scheme S1.

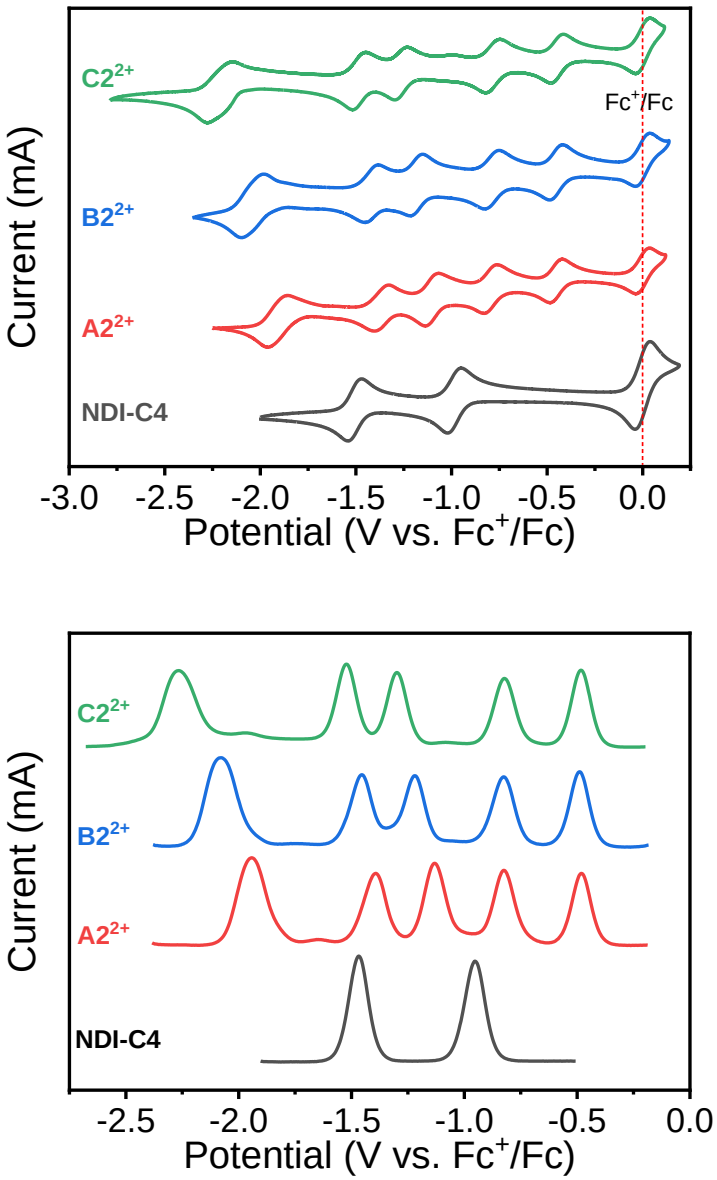

Figure S5. (Top) CVs and (bottom) DPVs of **A2²⁺**, **B2²⁺**, **C2²⁺** and **NDI-C4** in DMF solution (c = 1 mM), with 0.1 M $TBAPF_6$ as the electrolyte. The scan rate of CV was 100 mV s^{-1}. DPV parameters: Increase E = 4 mV, amplitude = 50 mV, pulse width = 60.0 ms, sampling width = 20.0 ms, pulse period = 500.0 ms. The structure of **NDI-C4** is shown in Scheme S1.

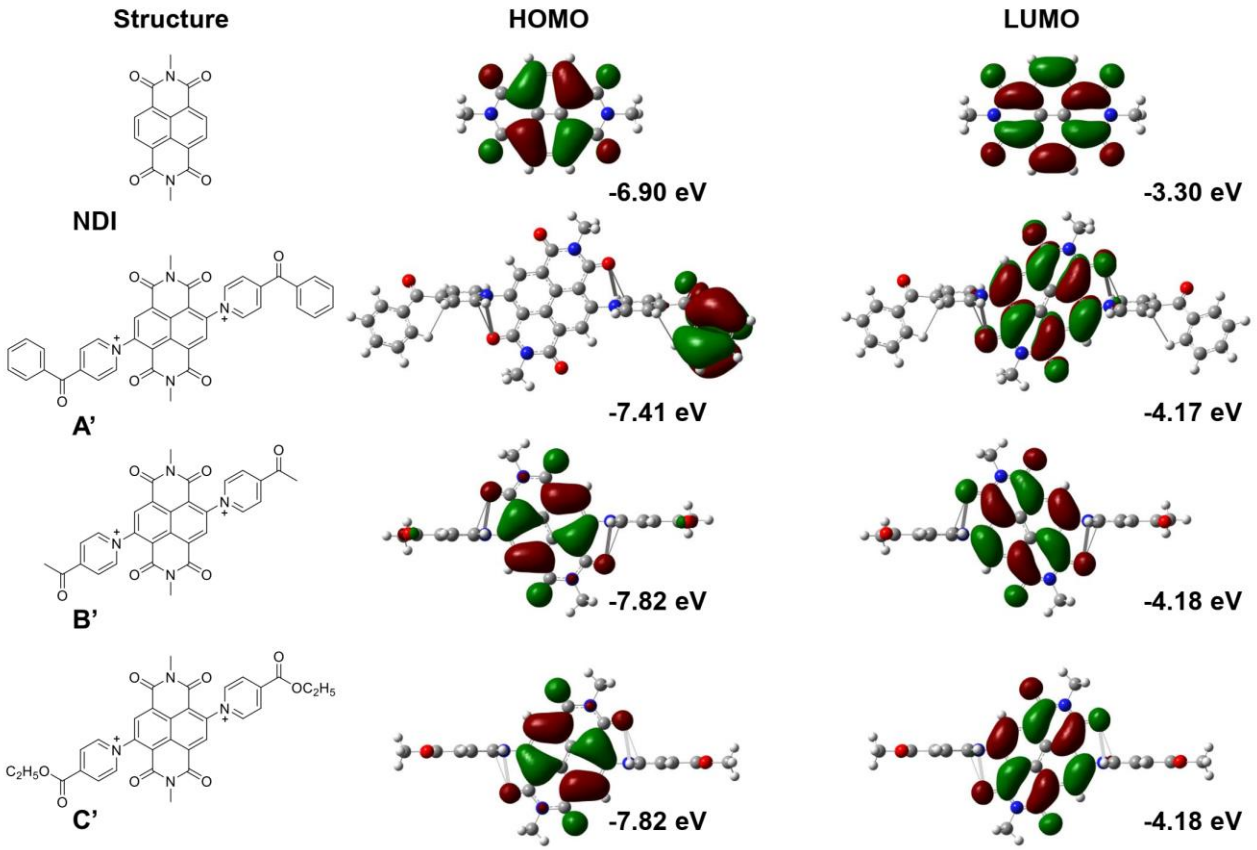

Figure S6. Structures of **NDI**, **A'**, **B'** and **C'**, as well as frontier molecular orbitals and their calculated energies.

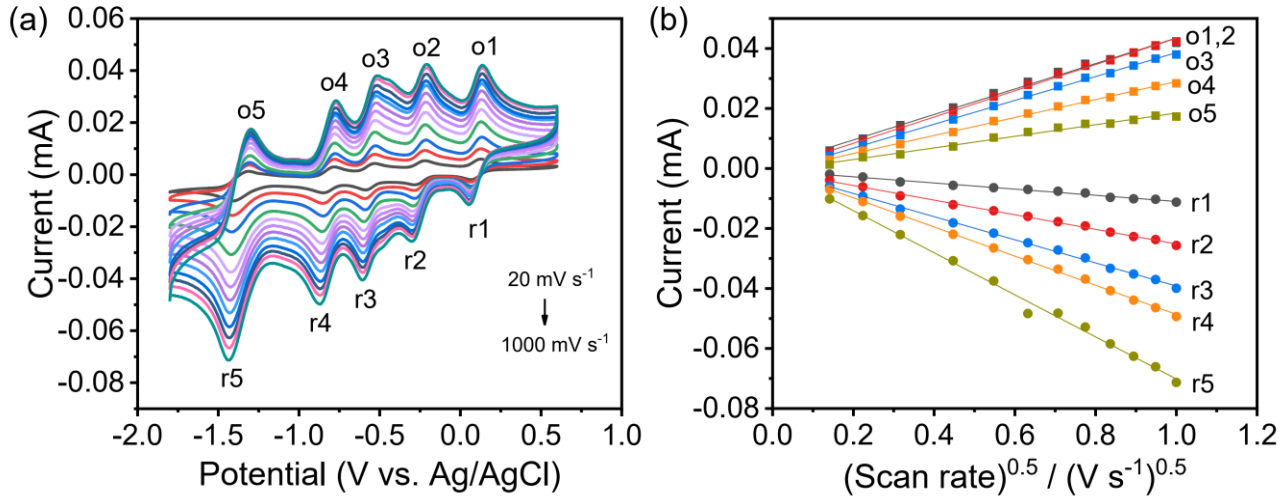

Figure S7. (a) Cyclic voltammograms of $\mathbf{A1}^{2+}$ (1 mM) in DMF solution at varying scan rates (20, 50, 100, 200, 300, 400, 500, 600, 700, 800, 900, 1000 mV s^{-1}; peak height increases with increasing scan rate). nBu$_4$PF$_6$ (0.1 M) as supporting electrolyte. (b) Linear plots of peak current *vs.* square root of the scan rate.

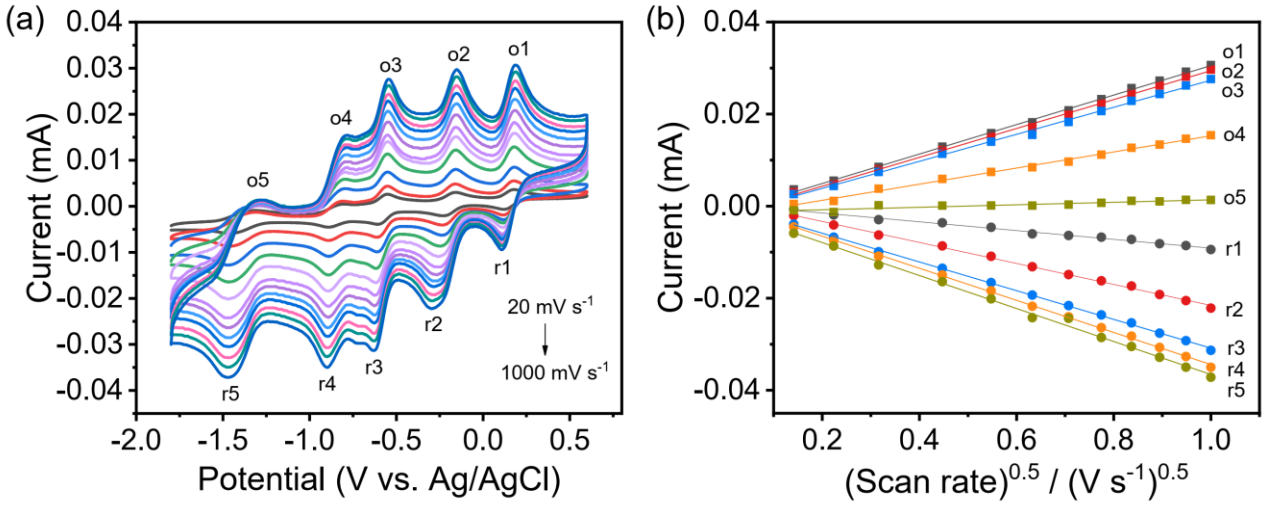

Figure S8. (a) Cyclic voltammograms of $\mathbf{B1}^{2+}$ (1 mM) in DMF solution at varying scan rates (20, 50, 100, 200, 300, 400, 500, 600, 700, 800, 900, 1000 mV s^{-1}; peak height increases with increasing scan rate). nBu$_4$PF$_6$ (0.1 M) as supporting electrolyte. (b) Linear plots of peak current *vs.* square root of the scan rate.

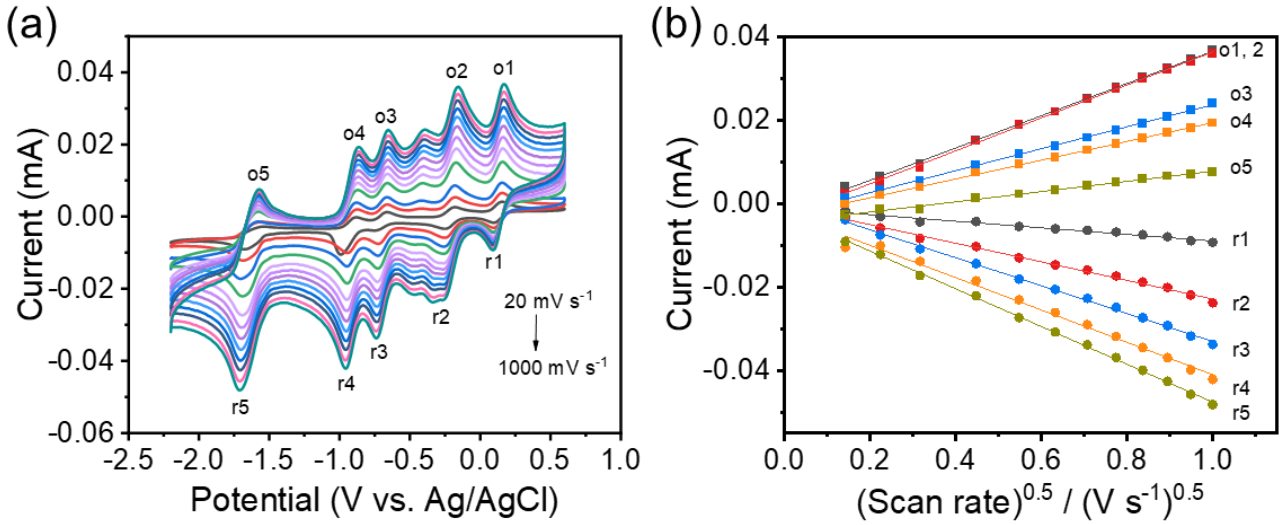

Figure S9. (a) Cyclic voltammograms of **C1**$^{2+}$ (1 mM) in DMF solution at varying scan rates (20, 50, 100, 200, 300, 400, 500, 600, 700, 800, 900, 1000 mV s^{-1}; peak height increases with increasing scan rate). nBu$_4$PF$_6$ (0.1 M) as supporting electrolyte. (b) Linear plots of peak current *vs.* square root of the scan rate.

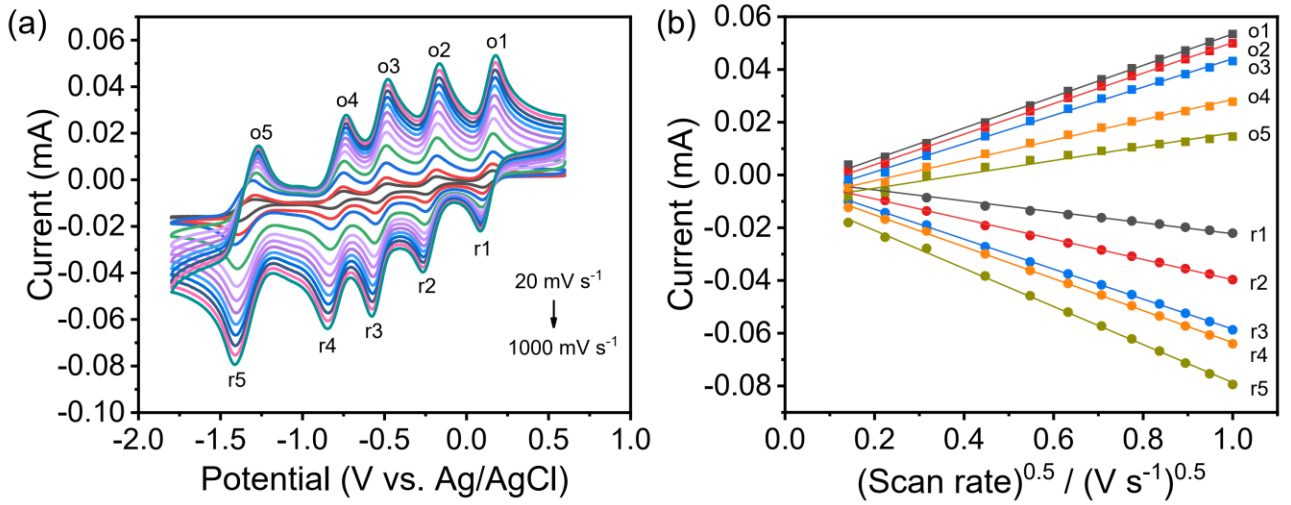

Figure S10. (a) Cyclic voltammograms of **A2**$^{2+}$ (1 mM) in DMF solution at varying scan rates (20, 50, 100, 200, 300, 400, 500, 600, 700, 800, 900, 1000 mV s^{-1}; peak height increases with increasing scan rate). nBu$_4$PF$_6$ (0.1 M) as supporting electrolyte. (b) Linear plots of peak current *vs.* square root of the scan rate.

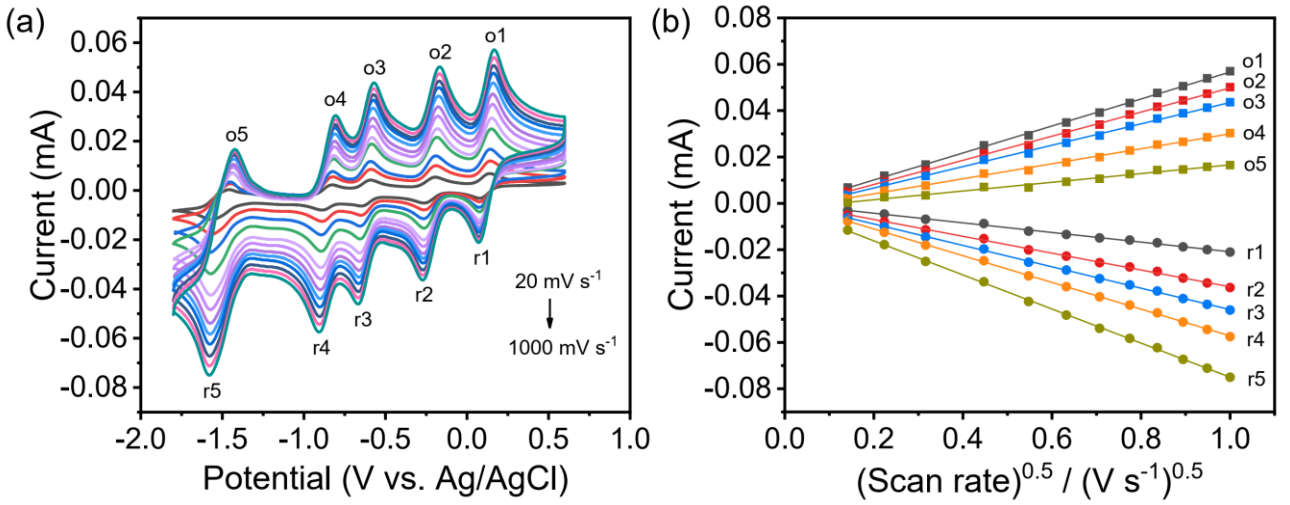

Figure S11. (a) Cyclic voltammograms of **B2**$^{2+}$ (1 mM) in DMF solution at varying scan rates (20, 50, 100, 200, 300, 400, 500, 600, 700, 800, 900, 1000 mV s^{-1}; peak height increases with increasing scan rate). *n*Bu_4PF_6 (0.1 M) as supporting electrolyte. (b) Linear plots of peak current *vs.* square root of the scan rate.

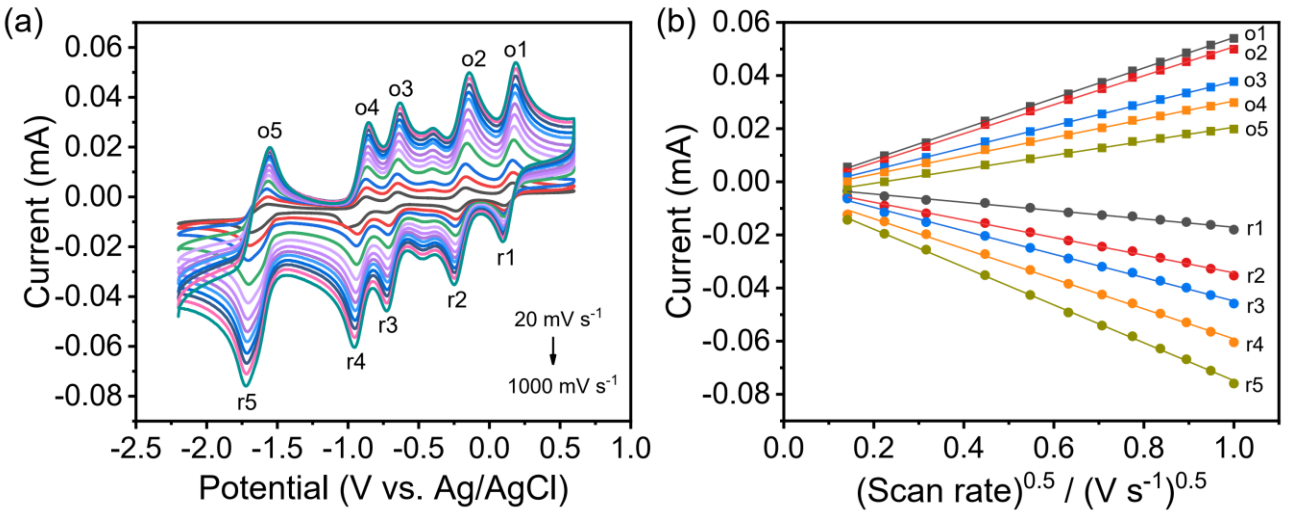

Figure S12. (a) Cyclic voltammograms of **C2**$^{2+}$ (1 mM) in DMF solution at varying scan rates (20, 50, 100, 200, 300, 400, 500, 600, 700, 800, 900, 1000 mV s^{-1}; peak height increases with increasing scan rate). *n*Bu_4PF_6 (0.1 M) as supporting electrolyte. (b) Linear plots of peak current *vs.* square root of the scan rate.

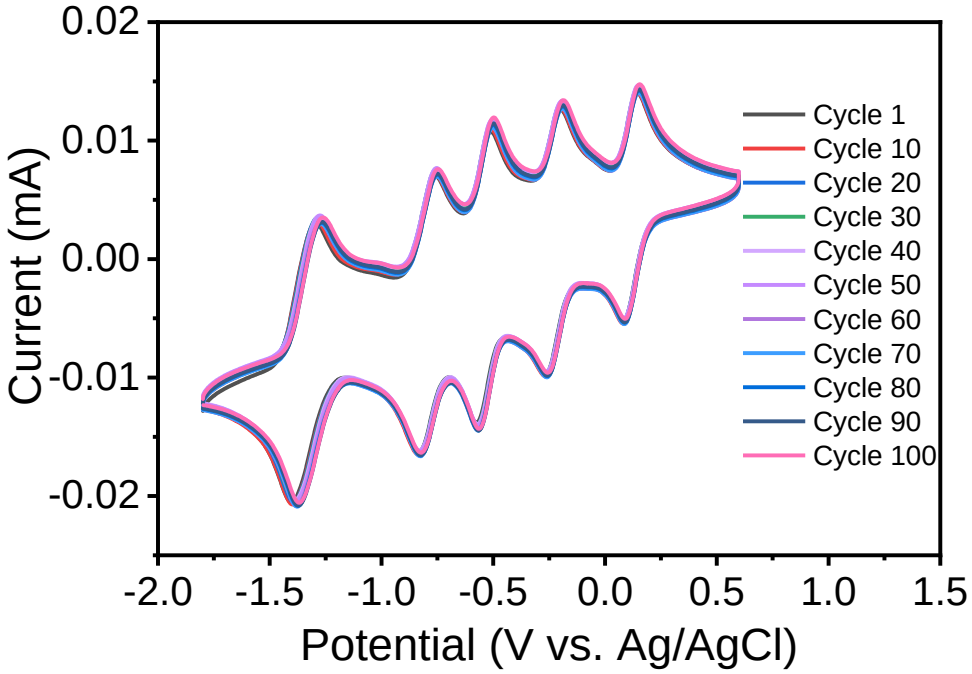

Figure S13. Test of electrochemical stability. CV curves of **A1**$^{2+}$ (1 mM) in degassed DMF solution with NBu_4PF_6 (0.1 M) as supporting electrolyte after 100 continuous cycles at a scan rate of 100 mV/s.

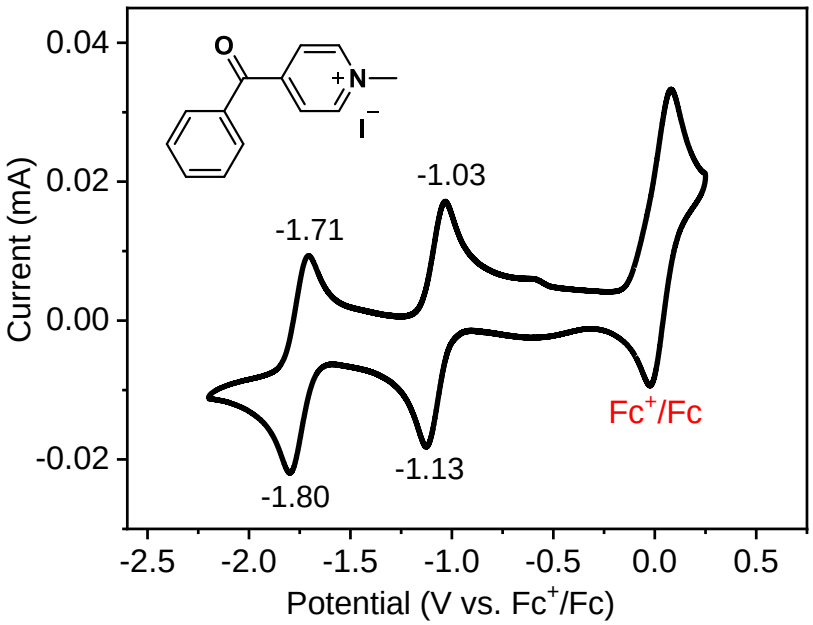

Figure S14. CV of **BMP** (1 mM) in DMF solution. NBu_4PF_6 (0.1 M) as supporting electrolyte; referenced vs. Fc^+/Fc. Inset shows the chemical structure of **BMP**.

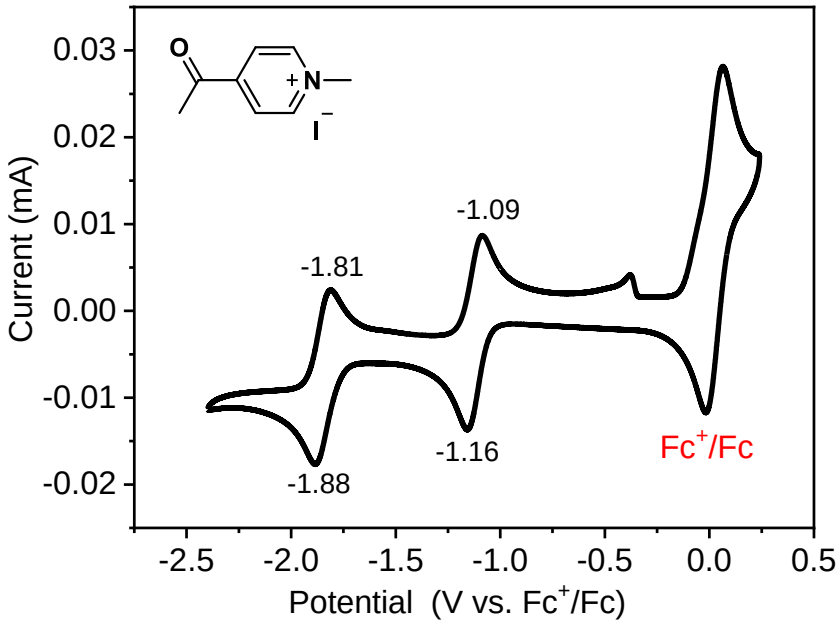

Figure S15. CV of **EMP** (1 mM) in DMF solution. NBu_4PF_6 (0.1 M) as supporting electrolyte; referenced vs. Fc^+/Fc. Inset shows the chemical structure of **EMP**.

Solubility Test

Their solubility was determined by UV spectrophotometry by soaking the compounds in G4 (tetraglyme) electrolyte for 24 h and then they were filtered before measurement (Figure S16). Based on the UV-vis data, the solubility follow the trend of **$(A2^{2+})Br_2$ < $(C2^{2+})Br_2$ < $(B2^{2+})Br_2$.**

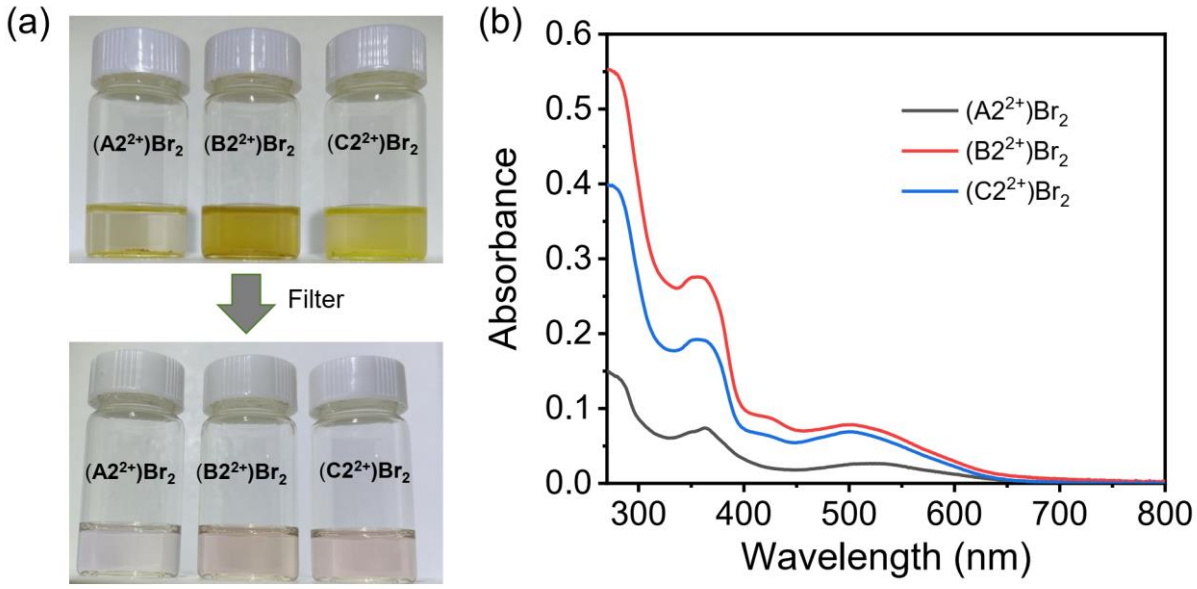

Figure S16. (a) The photographs of **$(A2^{2+})Br_2$**, **$(B2^{2+})Br_2$** and **$(C2^{2+})Br_2$** in electrolyte solution (G4, tetraglyme, 0.4 mg/mL) before and after filtering. (b) UV-vis spectra of **$(A2^{2+})Br_2$**, **$(B2^{2+})Br_2$** and **$(C2^{2+})Br_2$** in G4. The samples were soaked in G4 for 24 h before filtering and measurement.

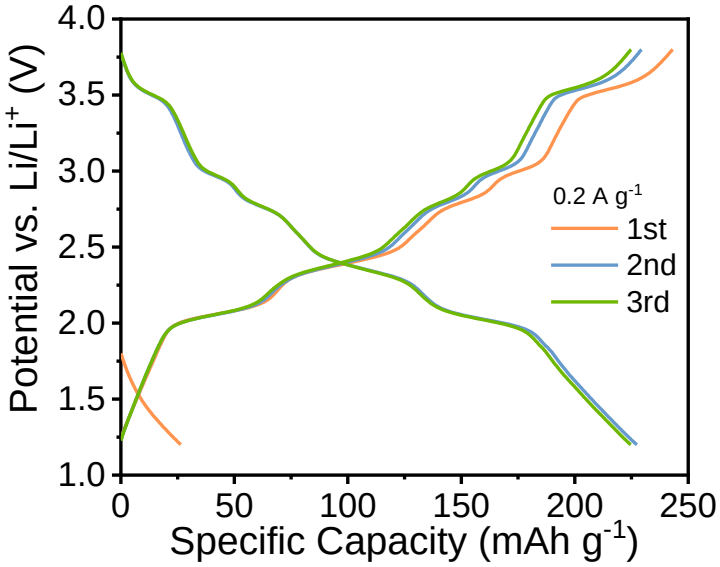

Figure S17. Galvanostatic charge-discharge profiles of **(A2^{2+})Br$_2$** during the first three cycles at 0.2 A g^{-1}.

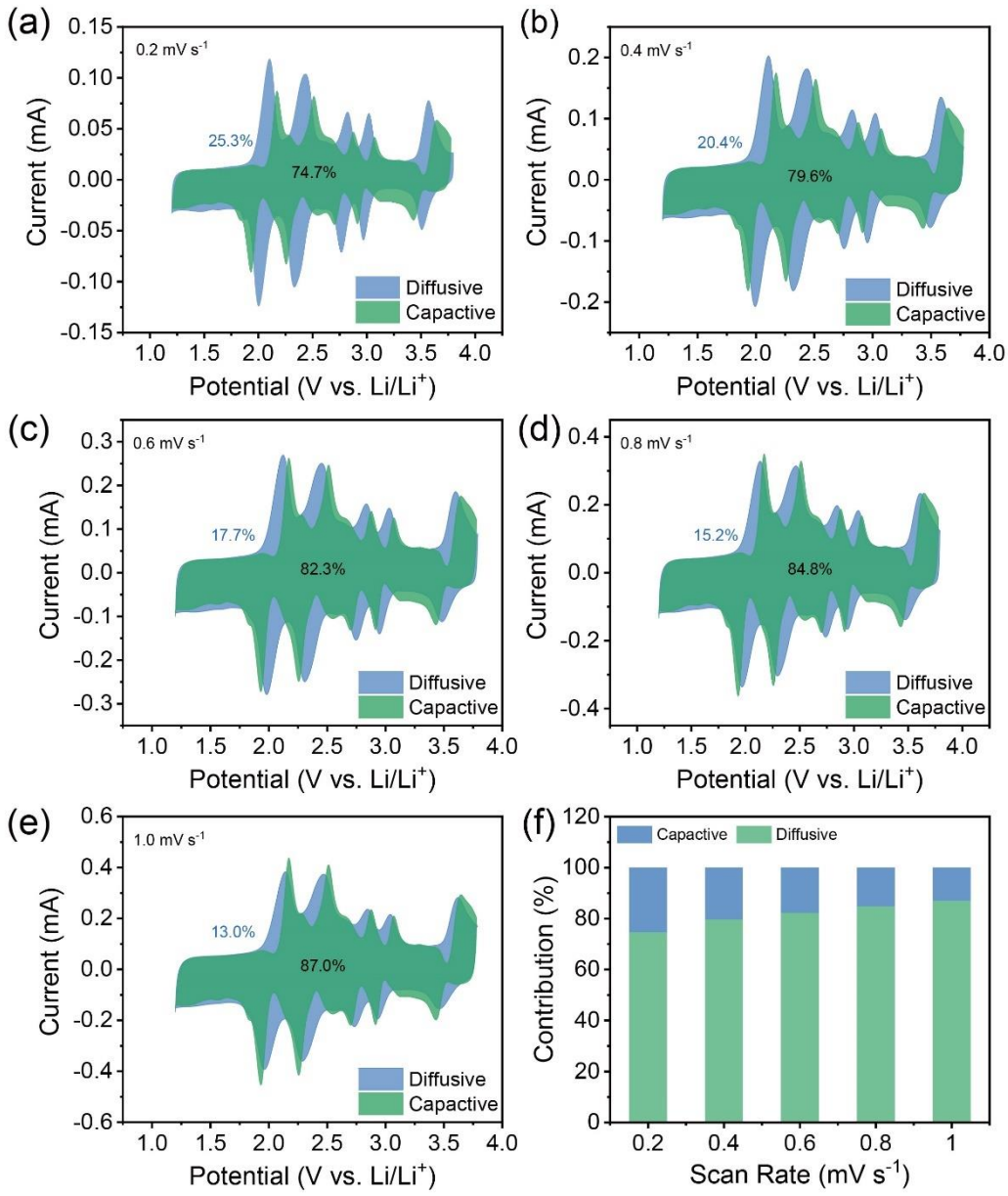

Figure S18. Capacitive and diffusive contributions of **[A2]Br2** at various scan rates.

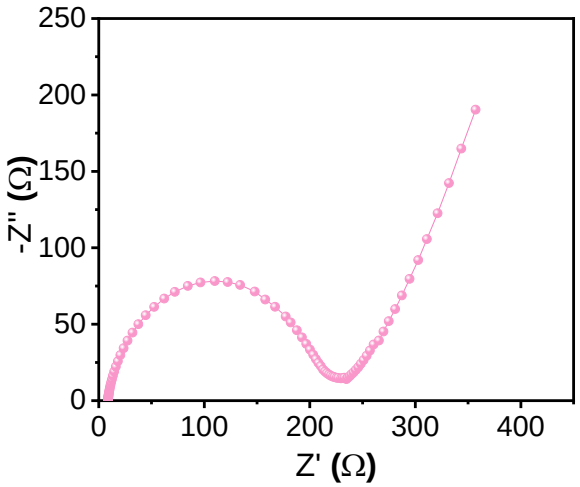

Figure S19. EIS spectra of **(A2^{2+})Br$_2$** electrodes before cycling.

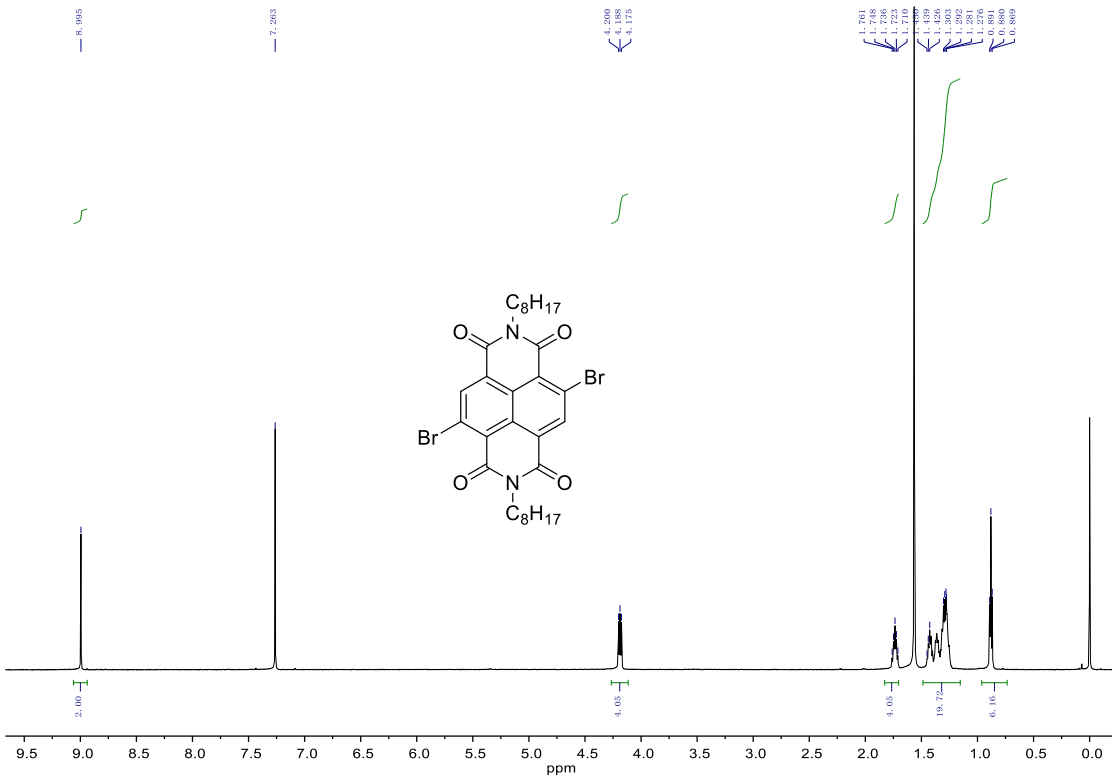

Figure S20. ^{1}H NMR spectrum of **S1** in $CDCl_3$.

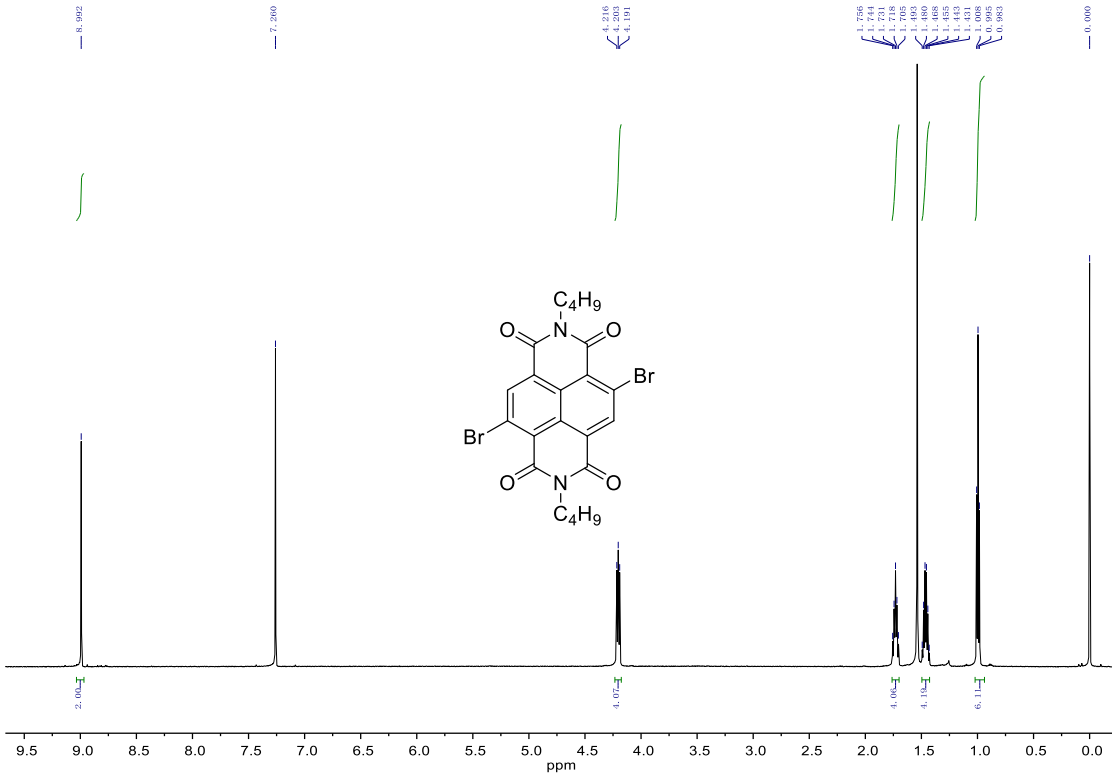

Figure S21. ^{1}H NMR spectrum of **S2** in $CDCl_3$.

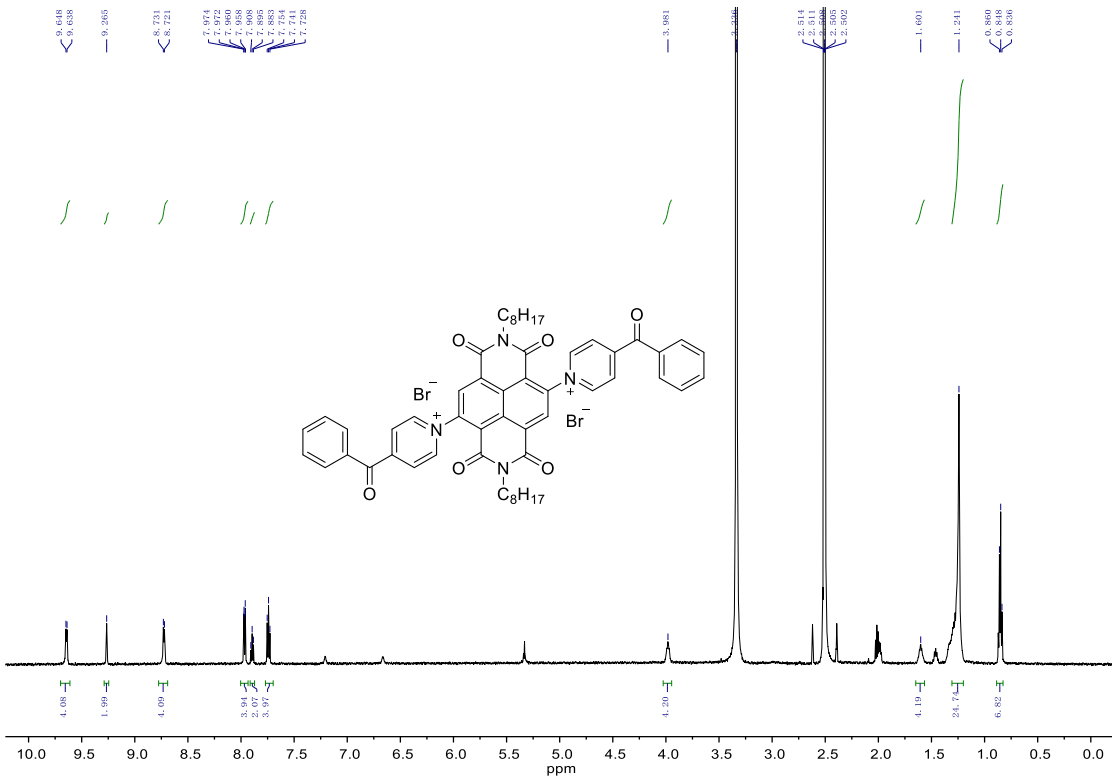

Figure S22. ^{1}H NMR spectrum of **(A1^{2+})Br$_2$** in d$_6$-DMSO.

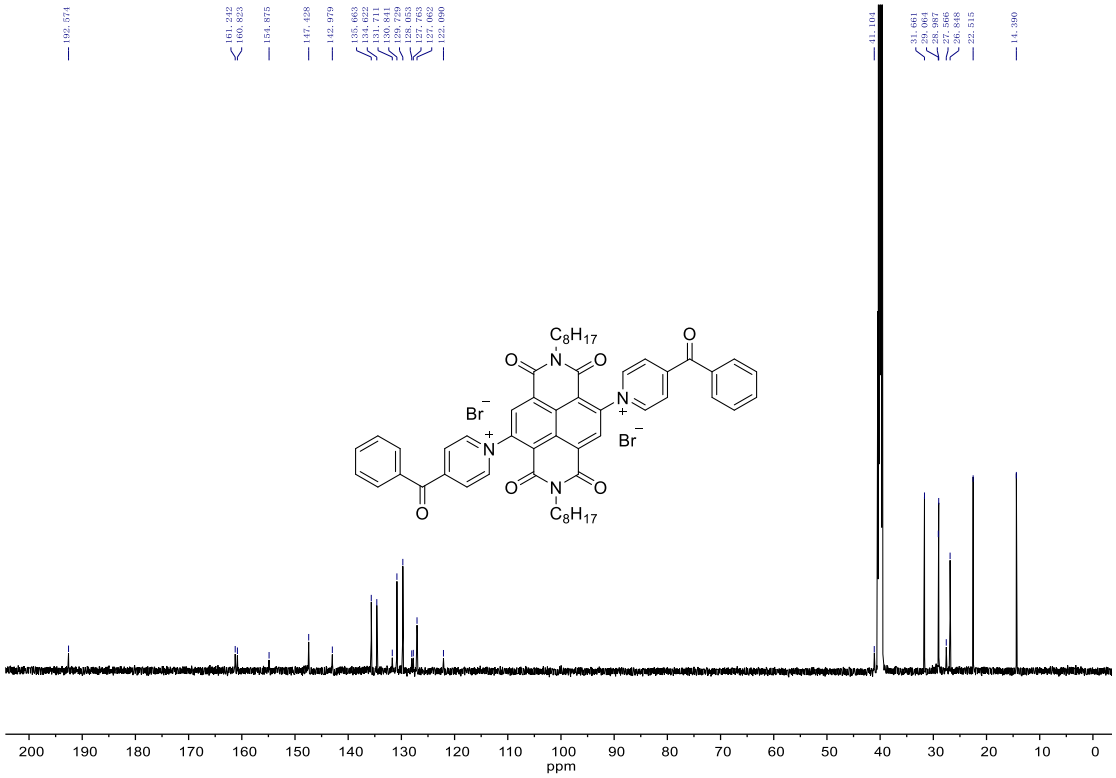

Figure S23. ^{13}C NMR spectrum of **(A1^{2+})Br$_2$** in d$_6$-DMSO.

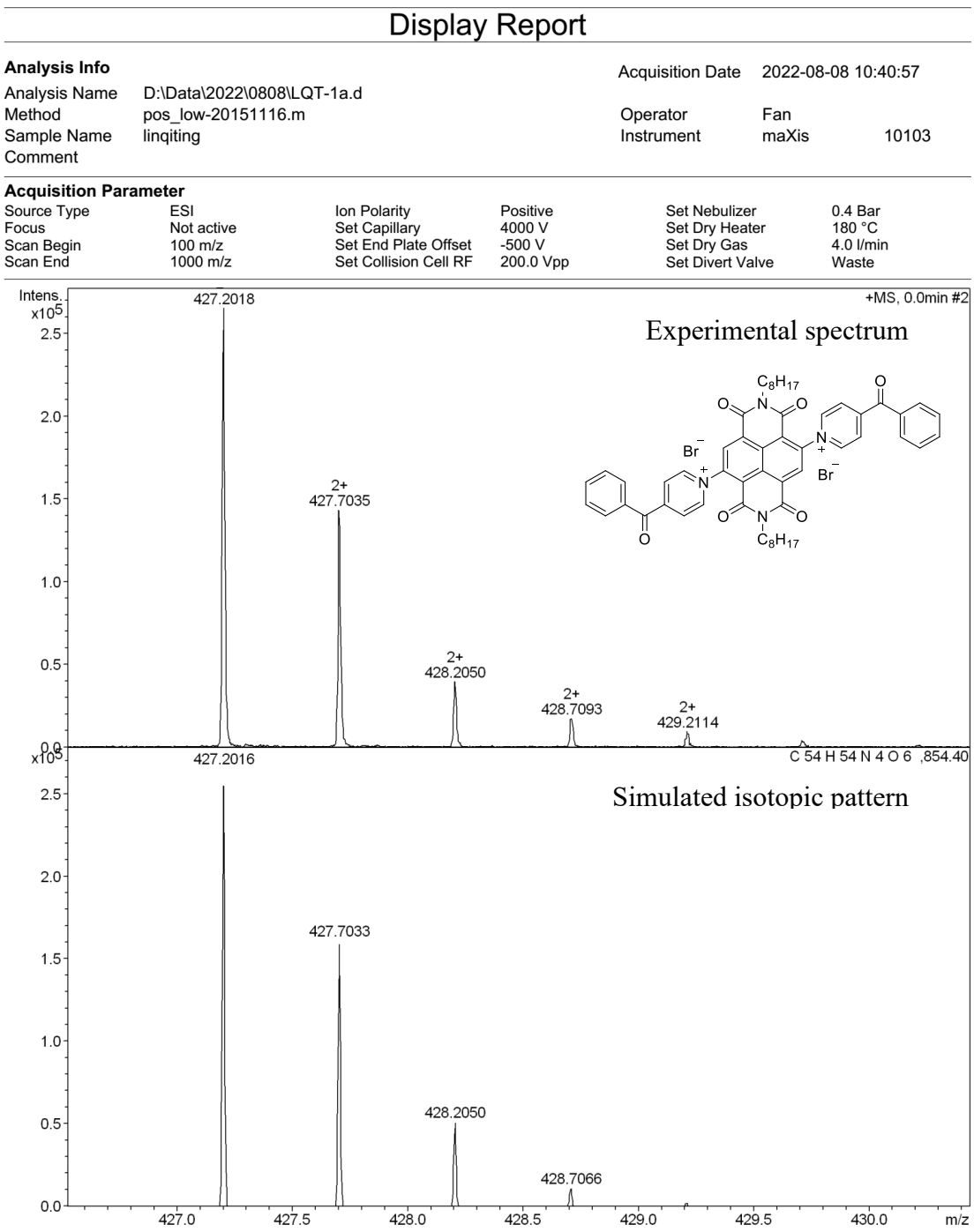

Figure S24. HRMS spectrum of **(A1^{2+})Br$_2$**.

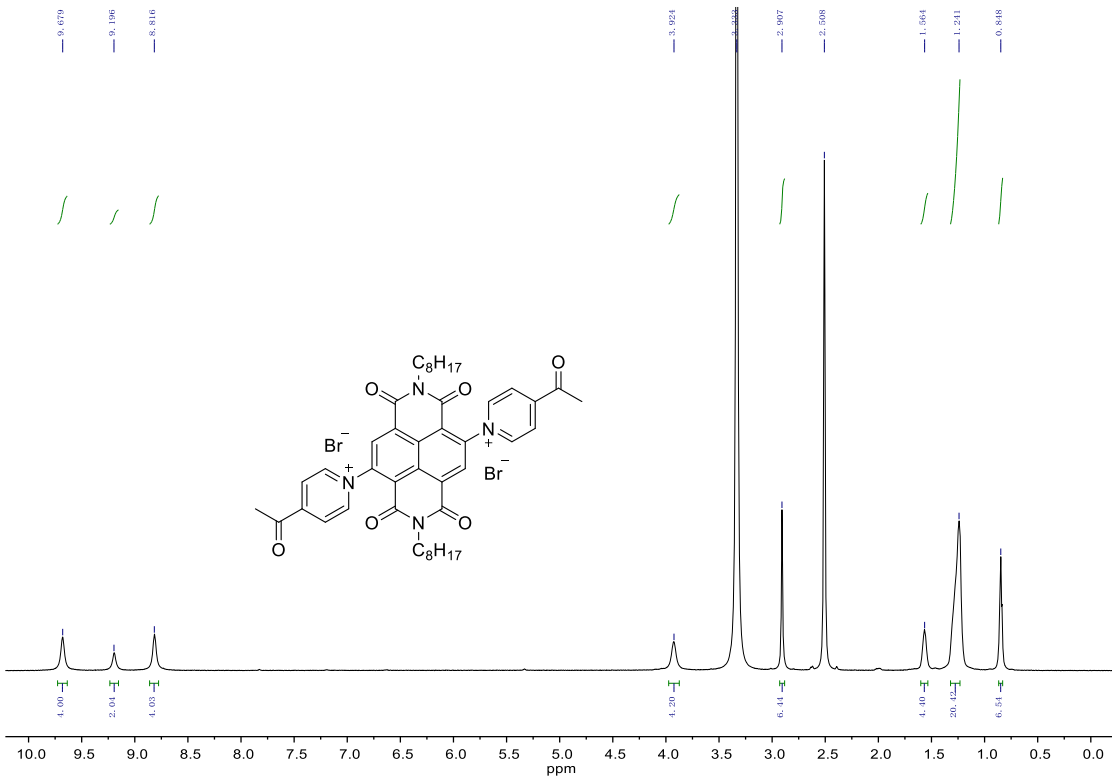

Figure S25. ^{1}H NMR spectrum of **(B1^{2+})Br$_2$** in d$_6$-DMSO.

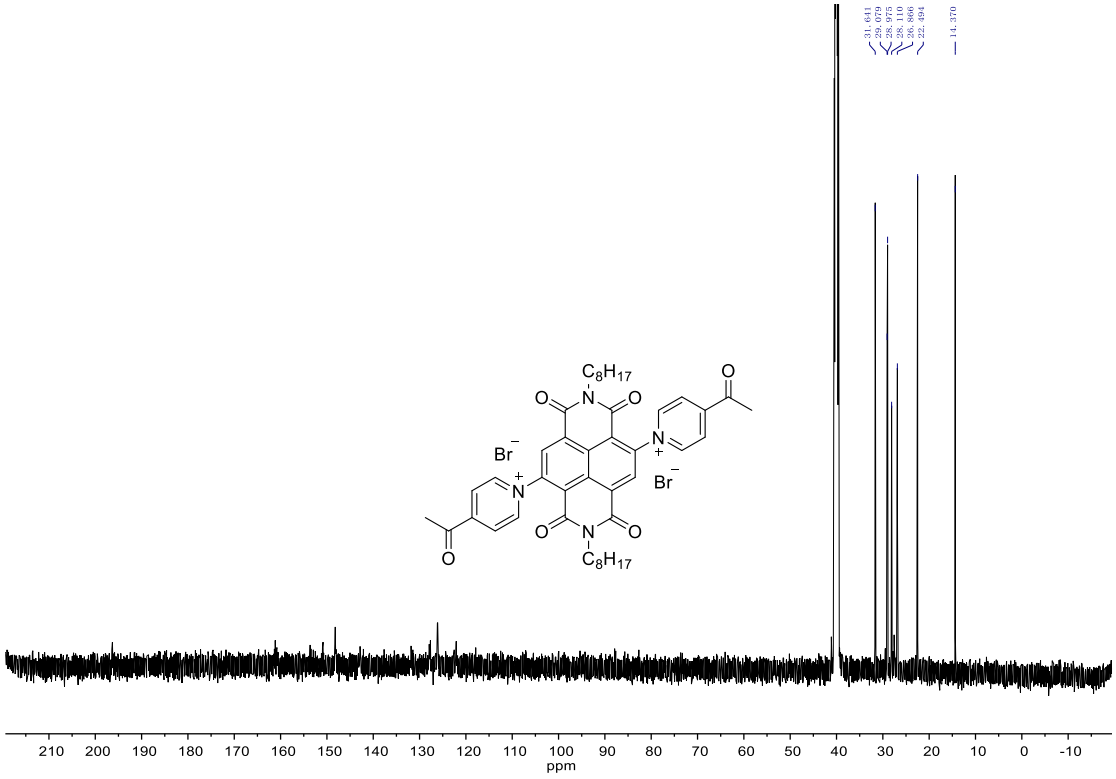

Figure S26. ^{13}C NMR spectrum of **(B1^{2+})Br$_2$** in d$_6$-DMSO.

Display Report

Analysis Info

Analysis Name	D:\Data\2022\0808\LQT-2.d	Acquisition Date	2022-08-08 10:43:48
Method	pos_low-20151116.m	Operator	Fan
Sample Name	linqiting	Instrument	maXis 10103
Comment			

Acquisition Parameter

Source Type	ESI	Ion Polarity	Positive	Set Nebulizer	0.4 Bar
Focus	Not active	Set Capillary	4000 V	Set Dry Heater	180 °C
Scan Begin	100 m/z	Set End Plate Offset	-500 V	Set Dry Gas	4.0 l/min
Scan End	1000 m/z	Set Collision Cell RF	200.0 Vpp	Set Divert Valve	Waste

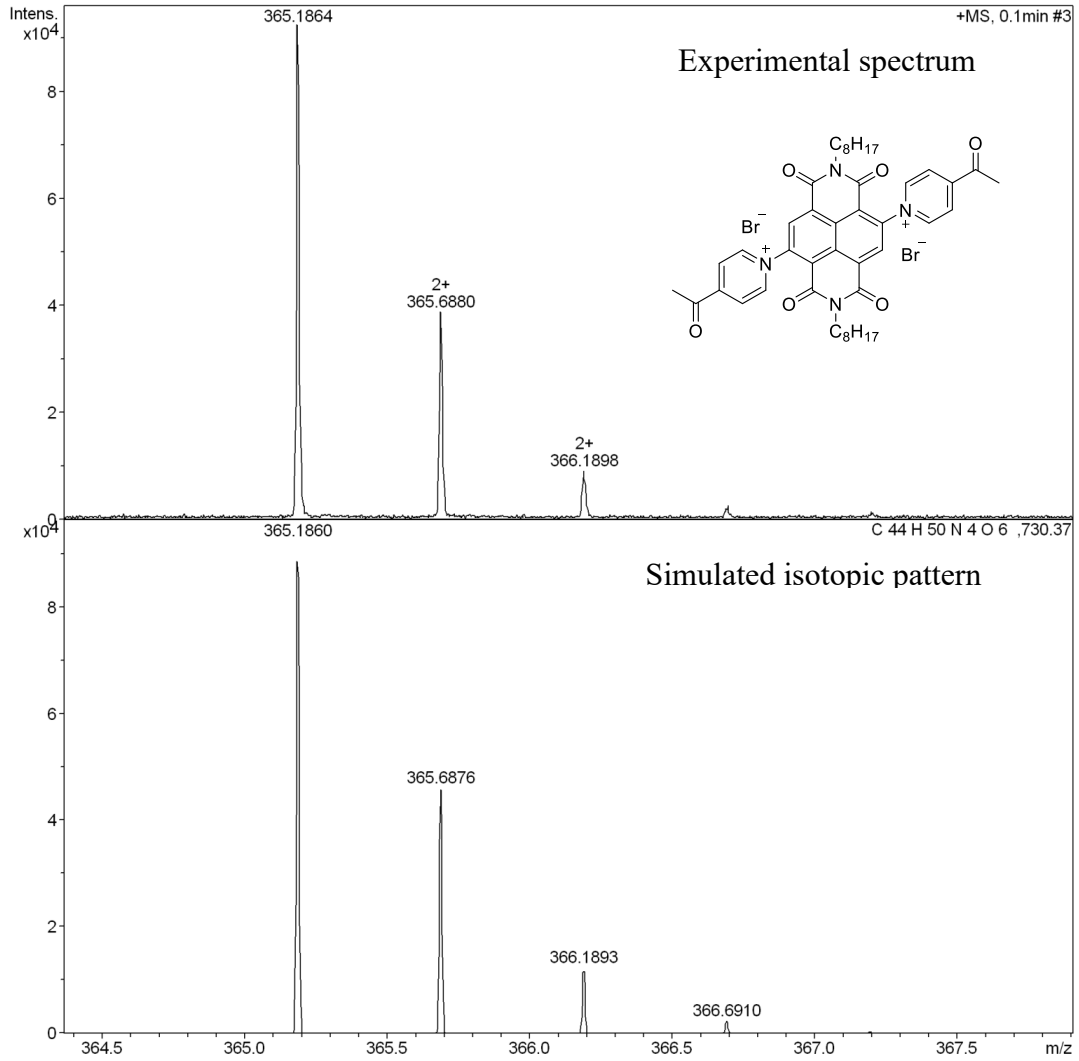

Figure S27. HRMS spectrum of **(B1^{2+})Br$_2$**.

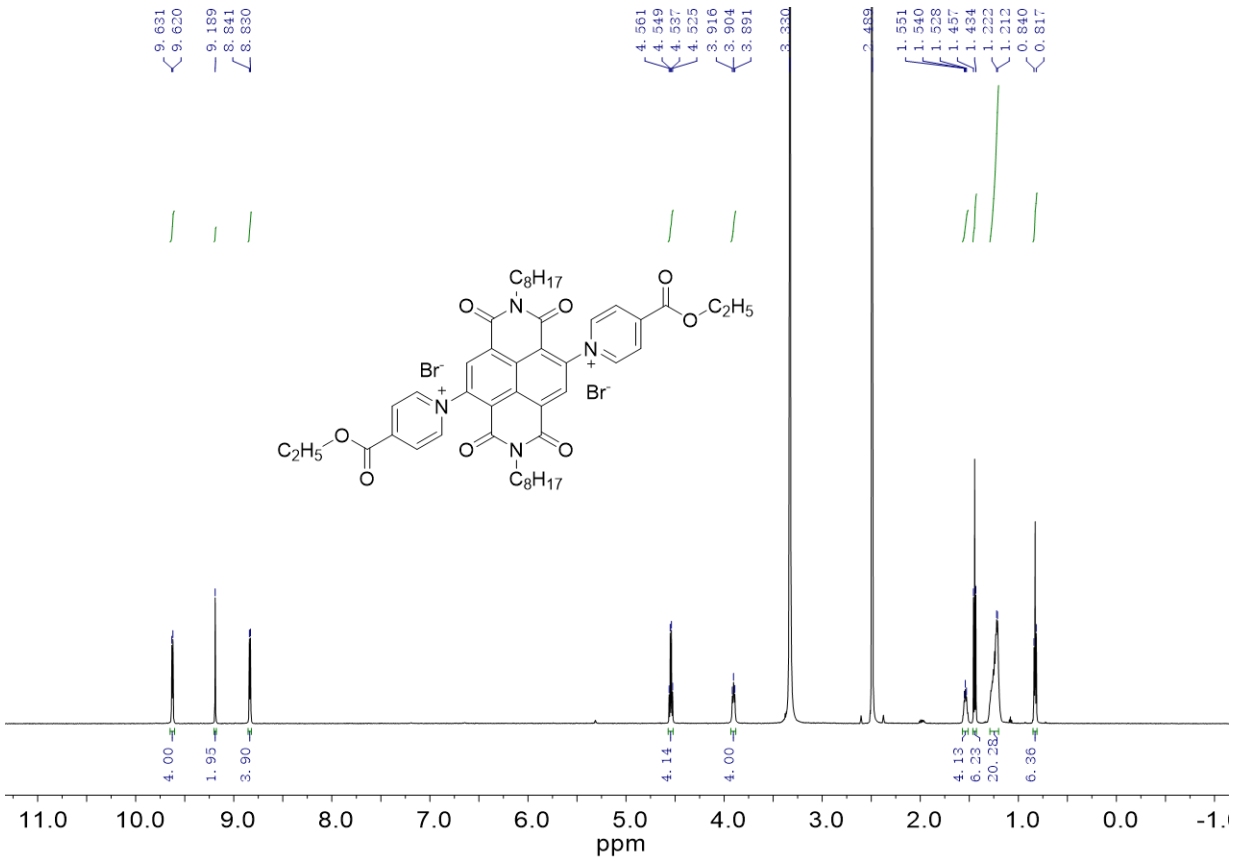

Figure S28. ^{1}H NMR spectrum of **(C1^{2+})Br$_2$** in d$_6$-DMSO.

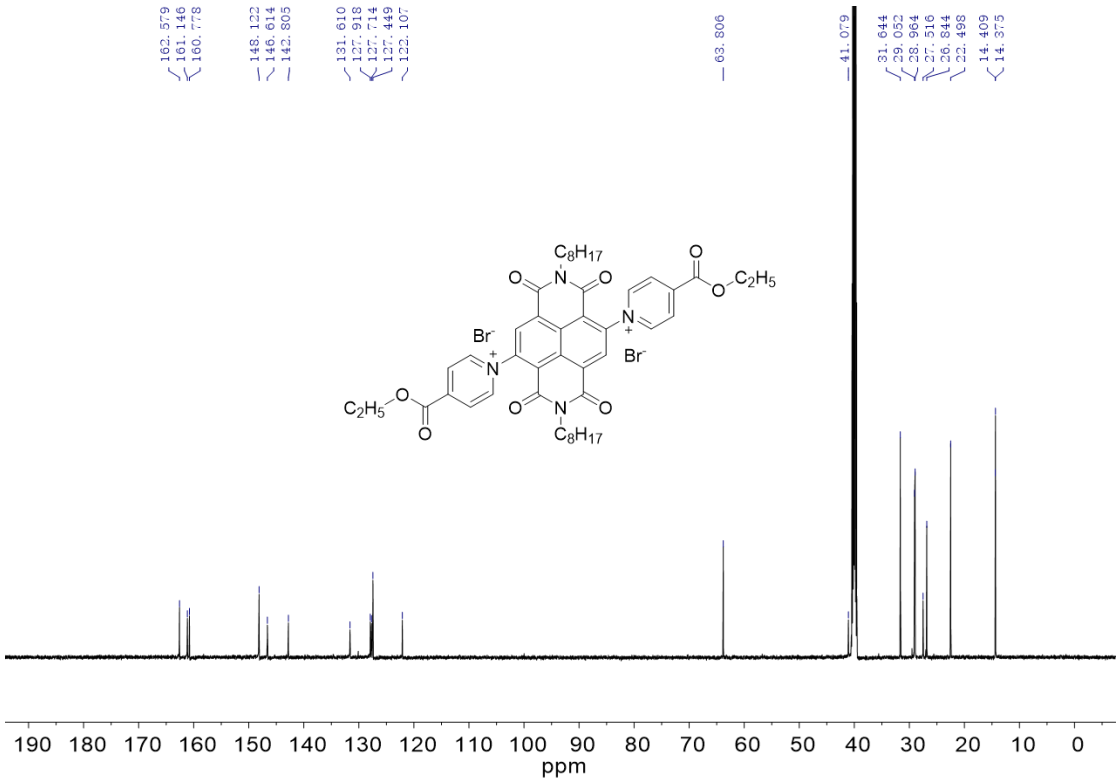

Figure S29. ^{13}C NMR spectrum of **(C1^{2+})Br$_2$** in d$_6$-DMSO.

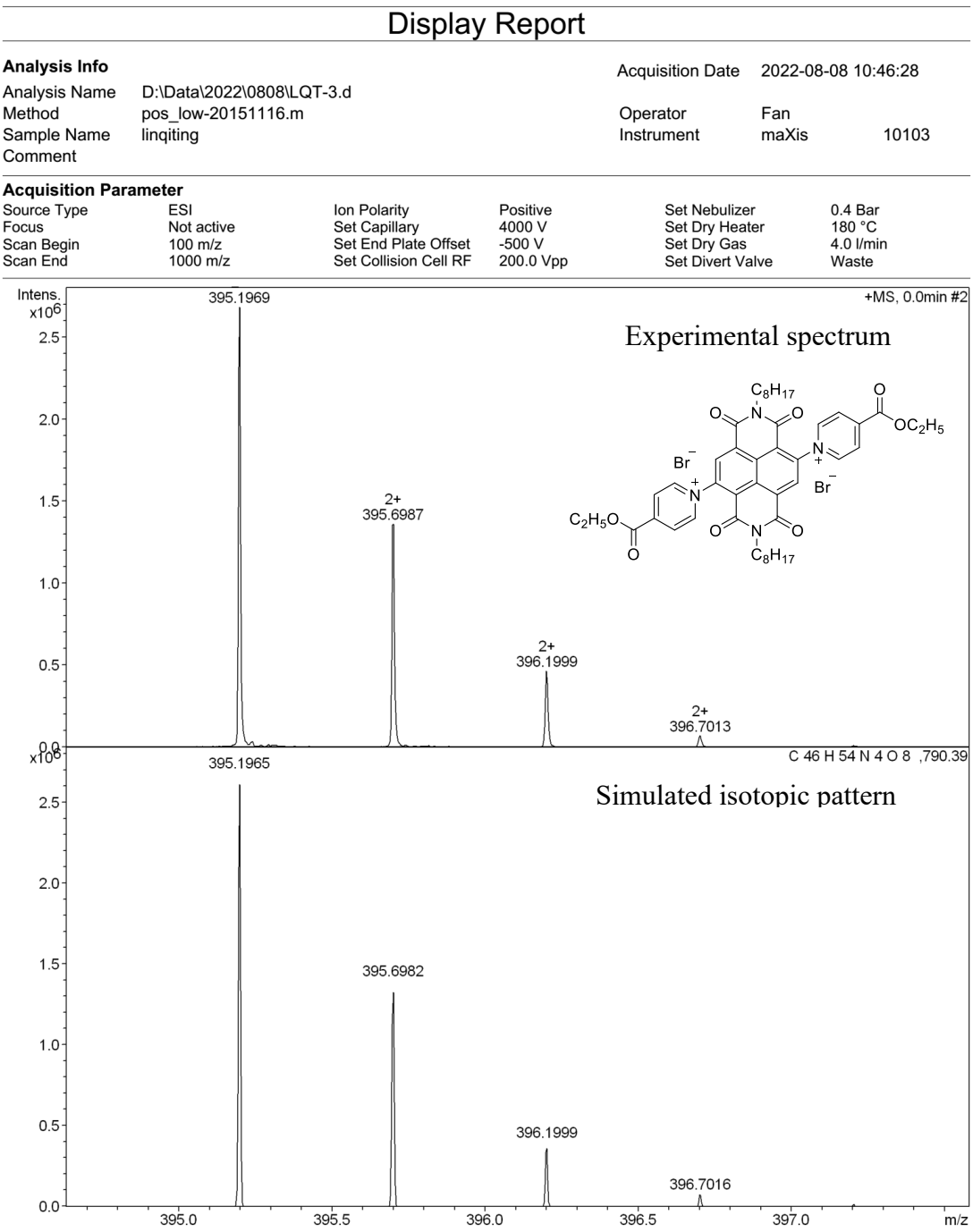

Figure S30. HRMS spectrum of **(C1^{2+})Br$_2$**.

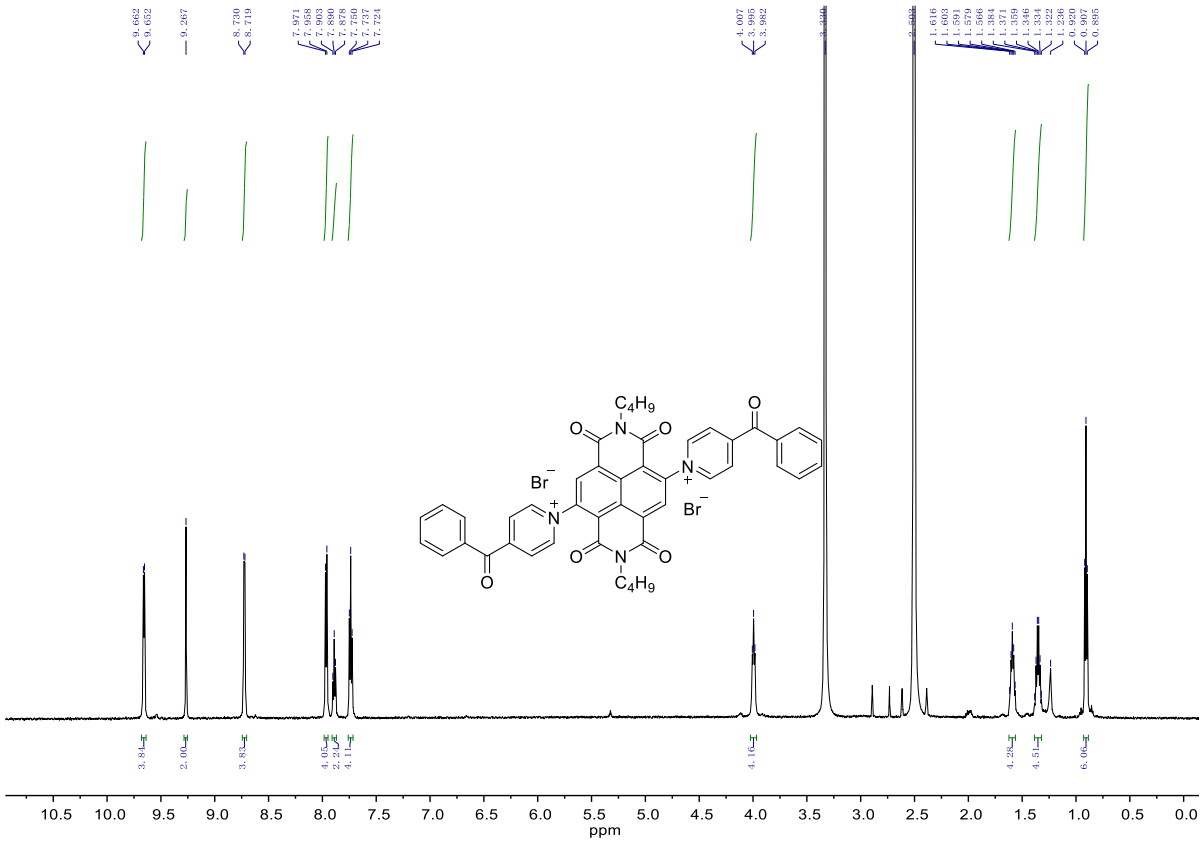

Figure S31. ^{1}H NMR spectrum of **(A2^{2+})Br$_2$** in d$_6$-DMSO.

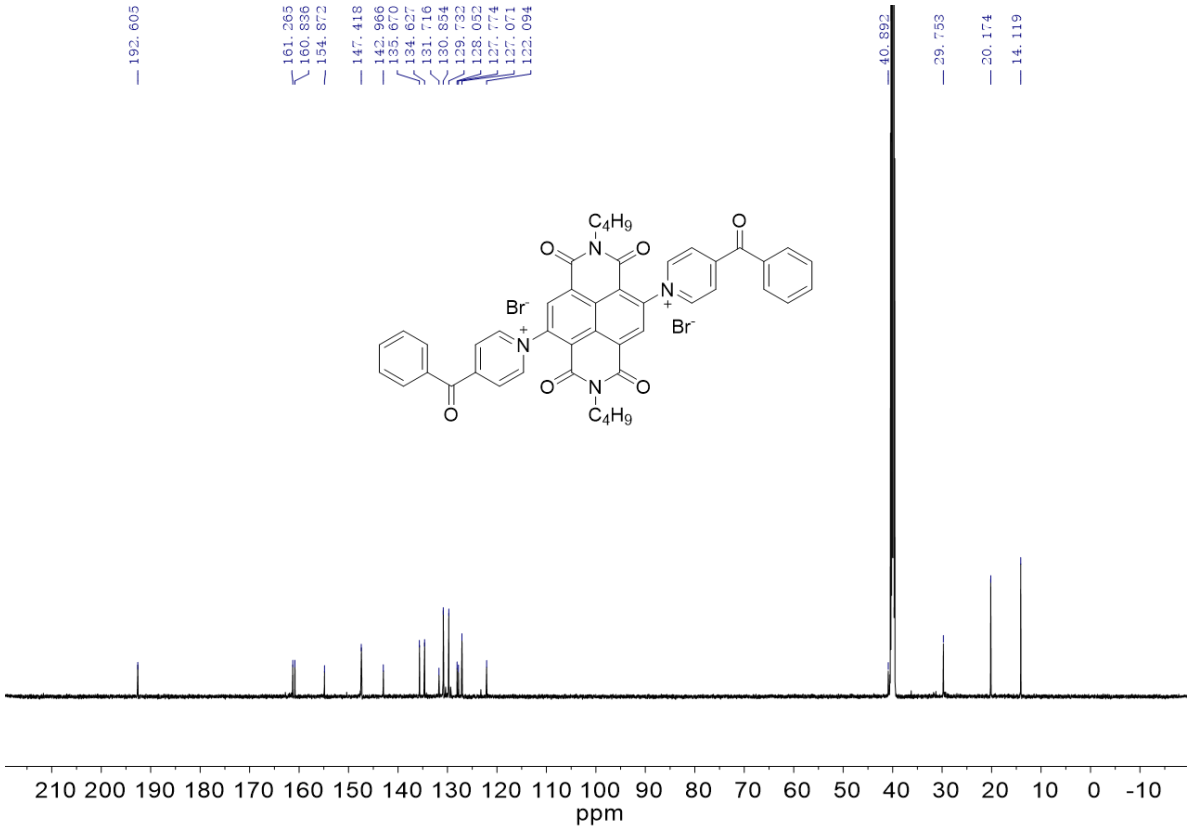

Figure S32. ^{13}C NMR spectrum of**(A2^{2+})Br$_2$** in d$_6$-DMSO.

Display Report

Analysis Info

Analysis Name	D:\Data\2022\1018\lqt-1-1.d	Acquisition Date	2022-10-18 10:03:46
Method	pos_low-20151116.m	Operator	Fan
Sample Name	linqiting	Instrument	maXis 10103
Comment			

Acquisition Parameter

Source Type	ESI	Ion Polarity	Positive	Set Nebulizer	0.4 Bar
Focus	Not active	Set Capillary	4000 V	Set Dry Heater	180 °C
Scan Begin	100 m/z	Set End Plate Offset	-500 V	Set Dry Gas	4.0 l/min
Scan End	1000 m/z	Set Collision Cell RF	200.0 Vpp	Set Divert Valve	Waste

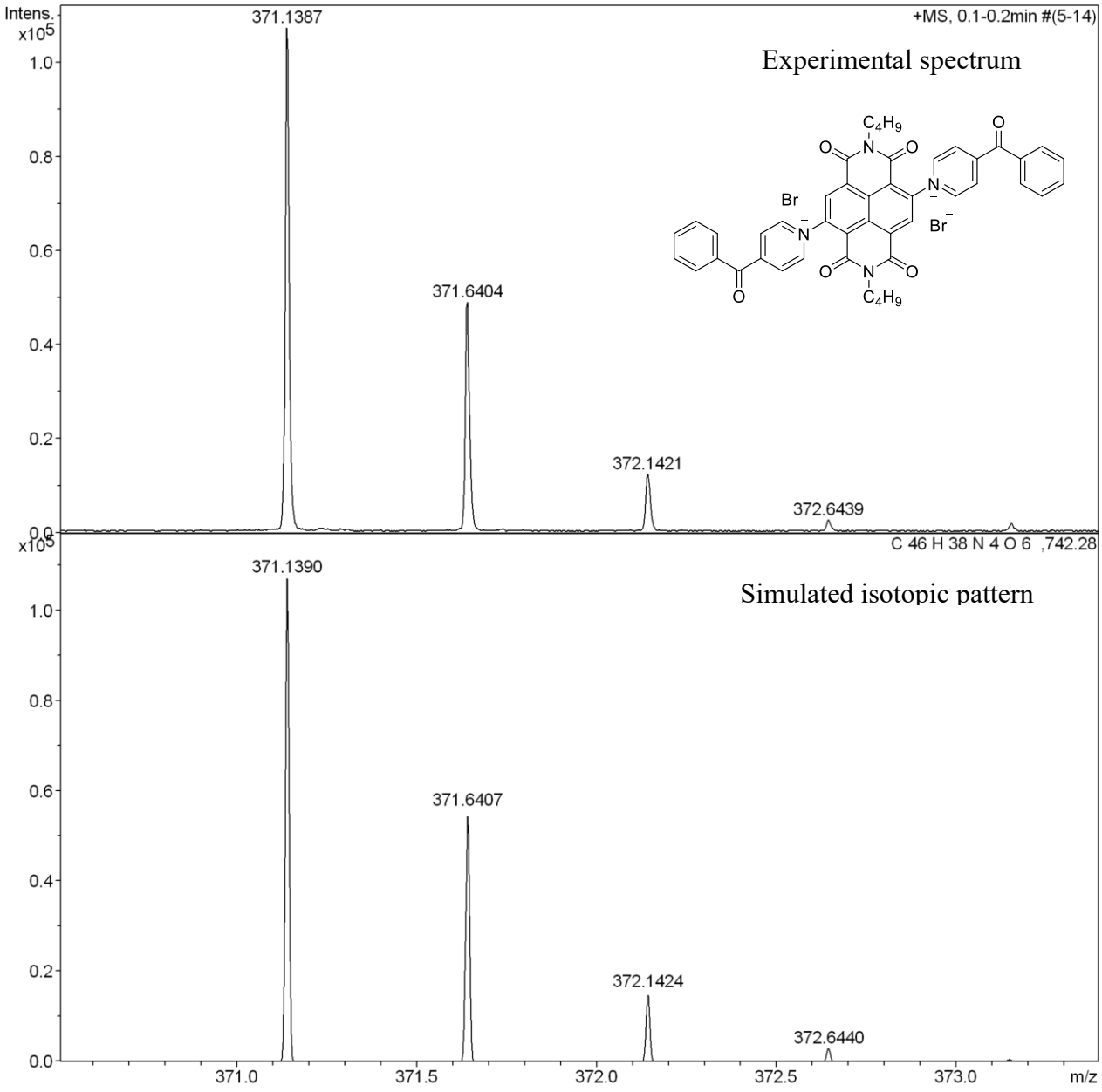

Figure S33. HRMS spectrum of **(A2^{2+})Br$_2$**.

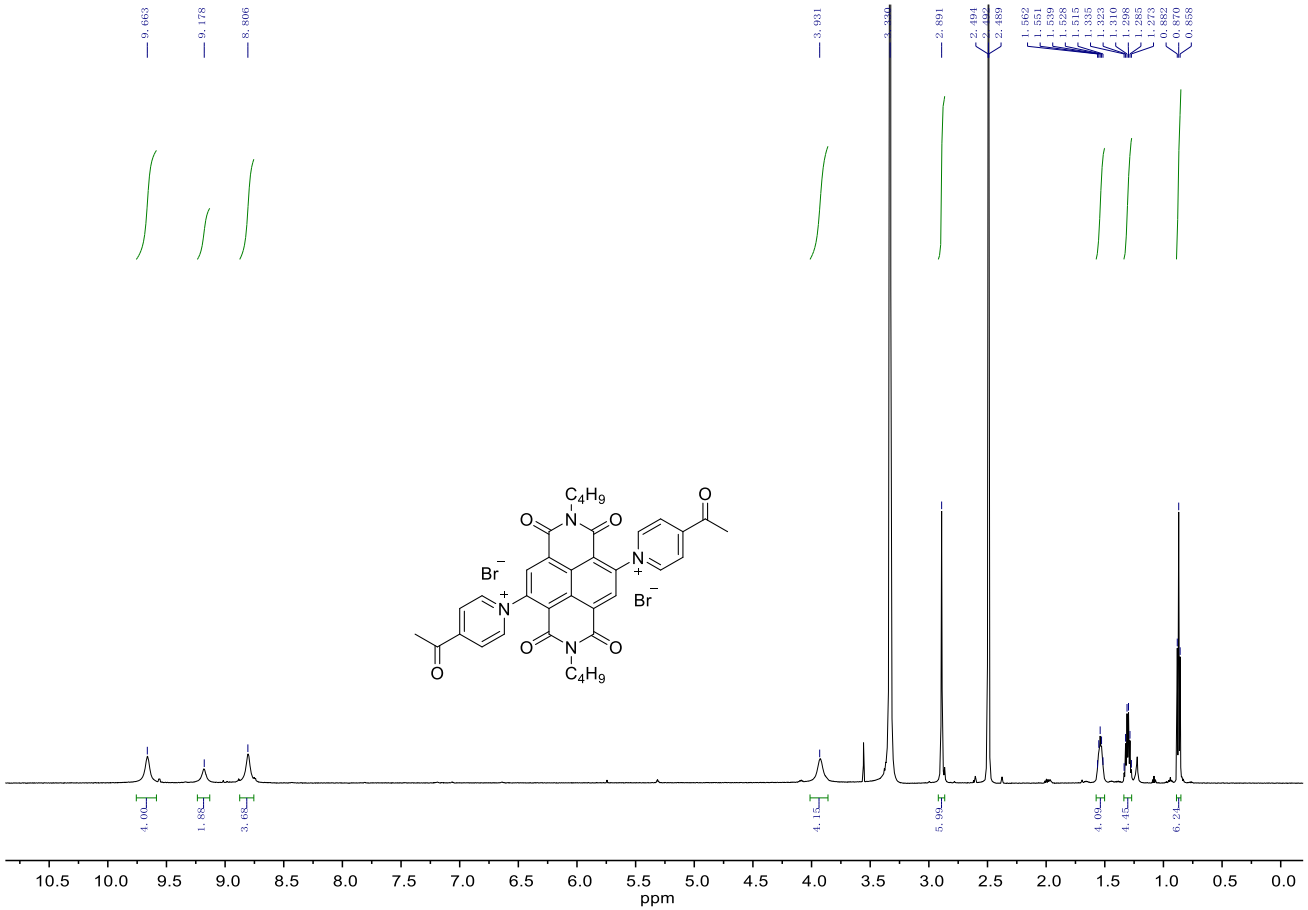

Figure S34. ^{1}H NMR spectrum of **(B2^{2+})Br$_2$** in d_6-DMSO.

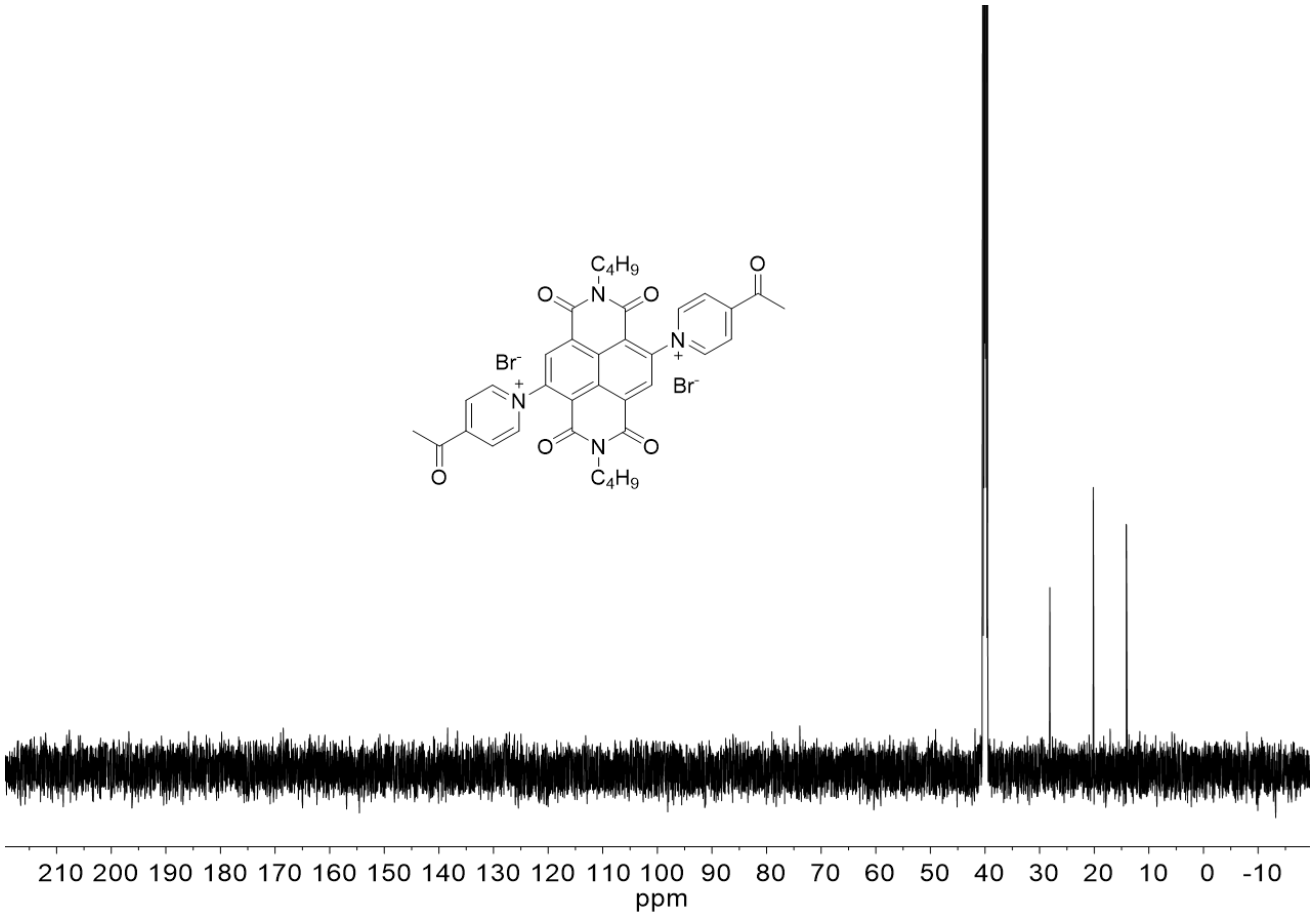

Figure S35. ^{13}C NMR spectrum of **(B2^{2+})Br$_2$** in d_6-DMSO.

Display Report

Analysis Info

Analysis Name	D:\Data\2022\1018\lqt-2.d	Acquisition Date	2022-10-18 10:07:15
Method	pos_low-20151116.m	Operator	Fan
Sample Name	linqiting	Instrument	maXis 10103
Comment			

Acquisition Parameter

Source Type	ESI	Ion Polarity	Positive	Set Nebulizer	0.4 Bar
Focus	Not active	Set Capillary	4000 V	Set Dry Heater	180 °C
Scan Begin	100 m/z	Set End Plate Offset	-500 V	Set Dry Gas	4.0 l/min
Scan End	1000 m/z	Set Collision Cell RF	200.0 Vpp	Set Divert Valve	Waste

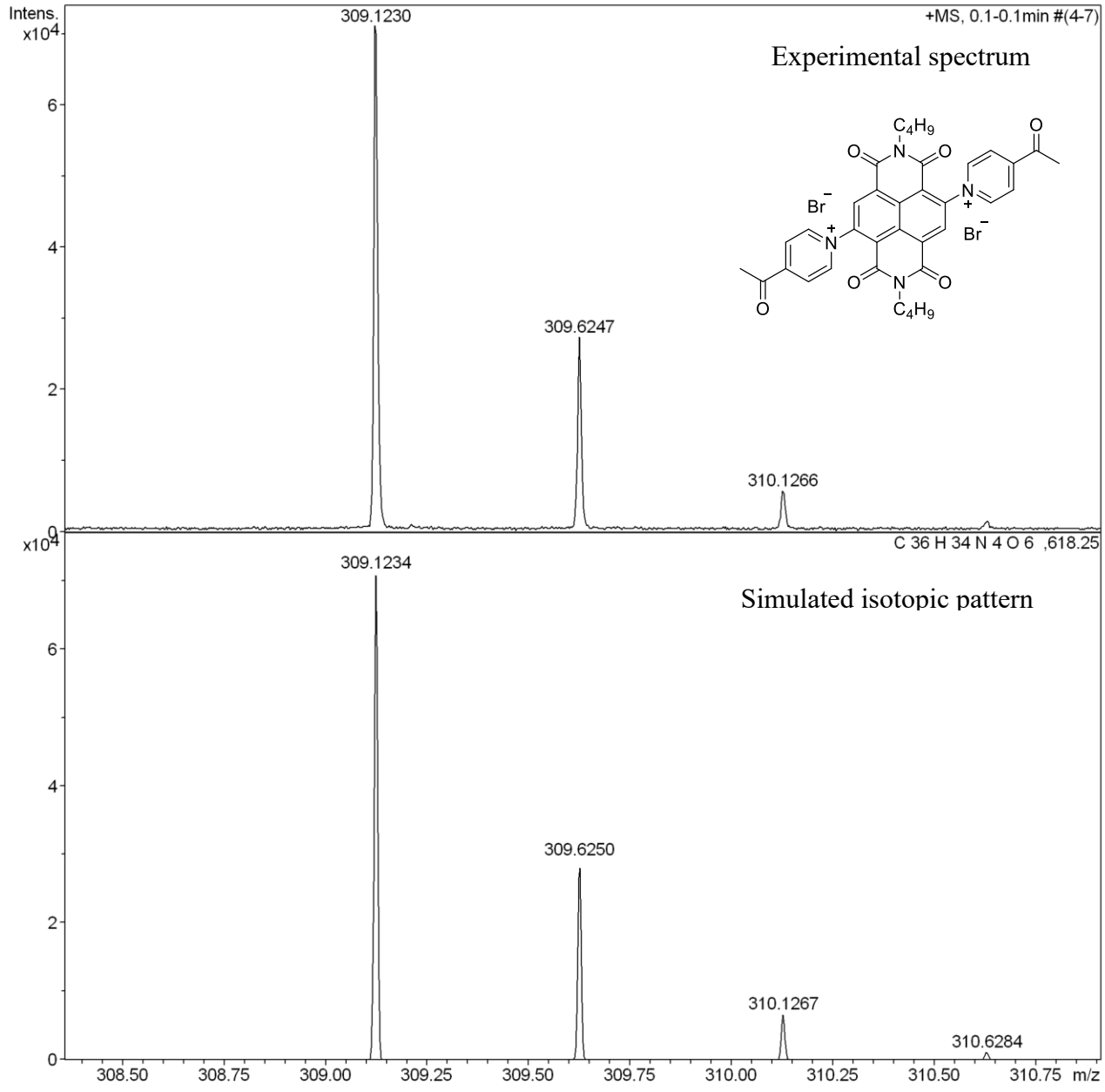

Figure S36. HRMS spectrum of **(B2^{2+})Br$_2$**.

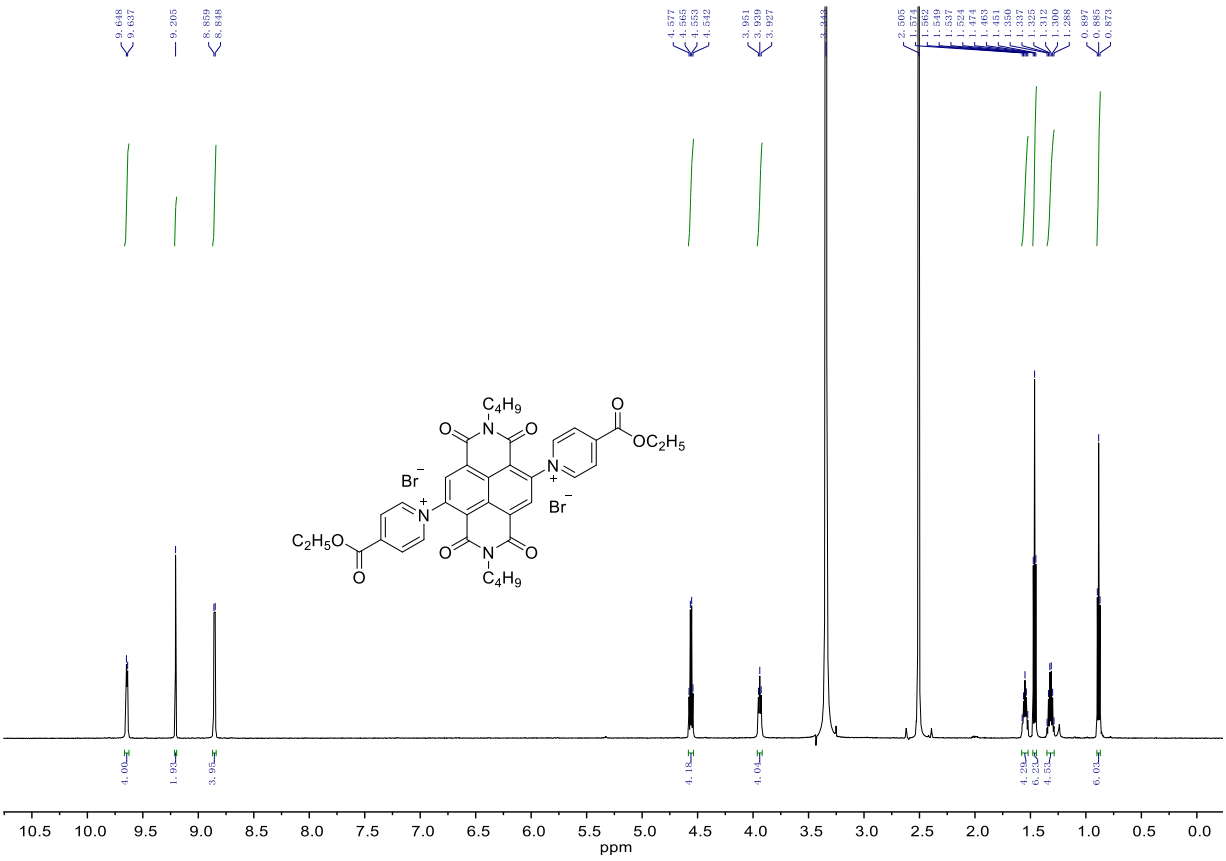

Figure S37. ^{1}H NMR spectrum of **(C2^{2+})Br$_2$** in d$_6$-DMSO.

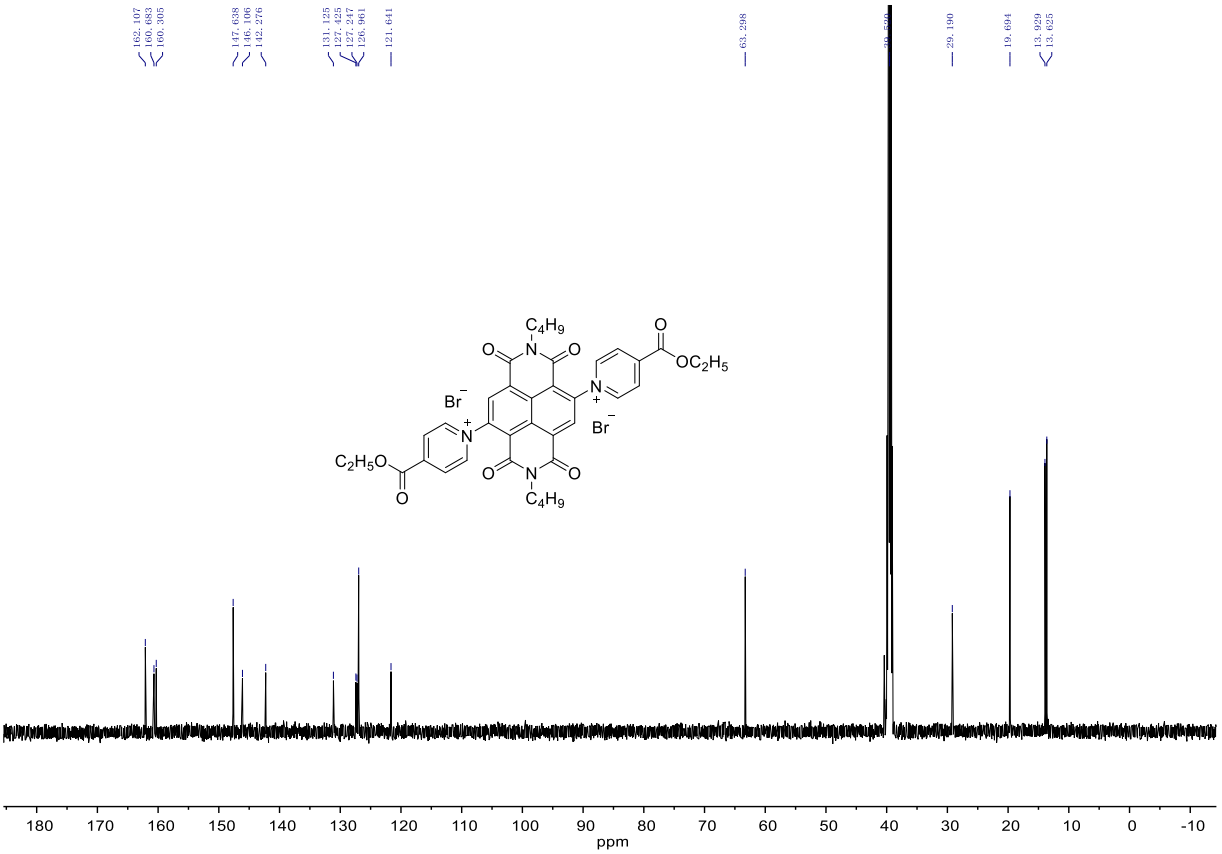

Figure S38. ^{13}C NMR spectrum of **(C2^{2+})Br$_2$** in d$_6$-DMSO.

Display Report

Analysis Info

Analysis Name	D:\Data\2022\1018\lqt-3.d	Acquisition Date	2022-10-18 10:10:04
Method	pos_low-20151116.m	Operator	Fan
Sample Name	linqiting	Instrument	maXis 10103
Comment			

Acquisition Parameter

Source Type	ESI	Ion Polarity	Positive	Set Nebulizer	0.4 Bar
Focus	Not active	Set Capillary	4000 V	Set Dry Heater	180 °C
Scan Begin	100 m/z	Set End Plate Offset	-500 V	Set Dry Gas	4.0 l/min
Scan End	1000 m/z	Set Collision Cell RF	200.0 Vpp	Set Divert Valve	Waste

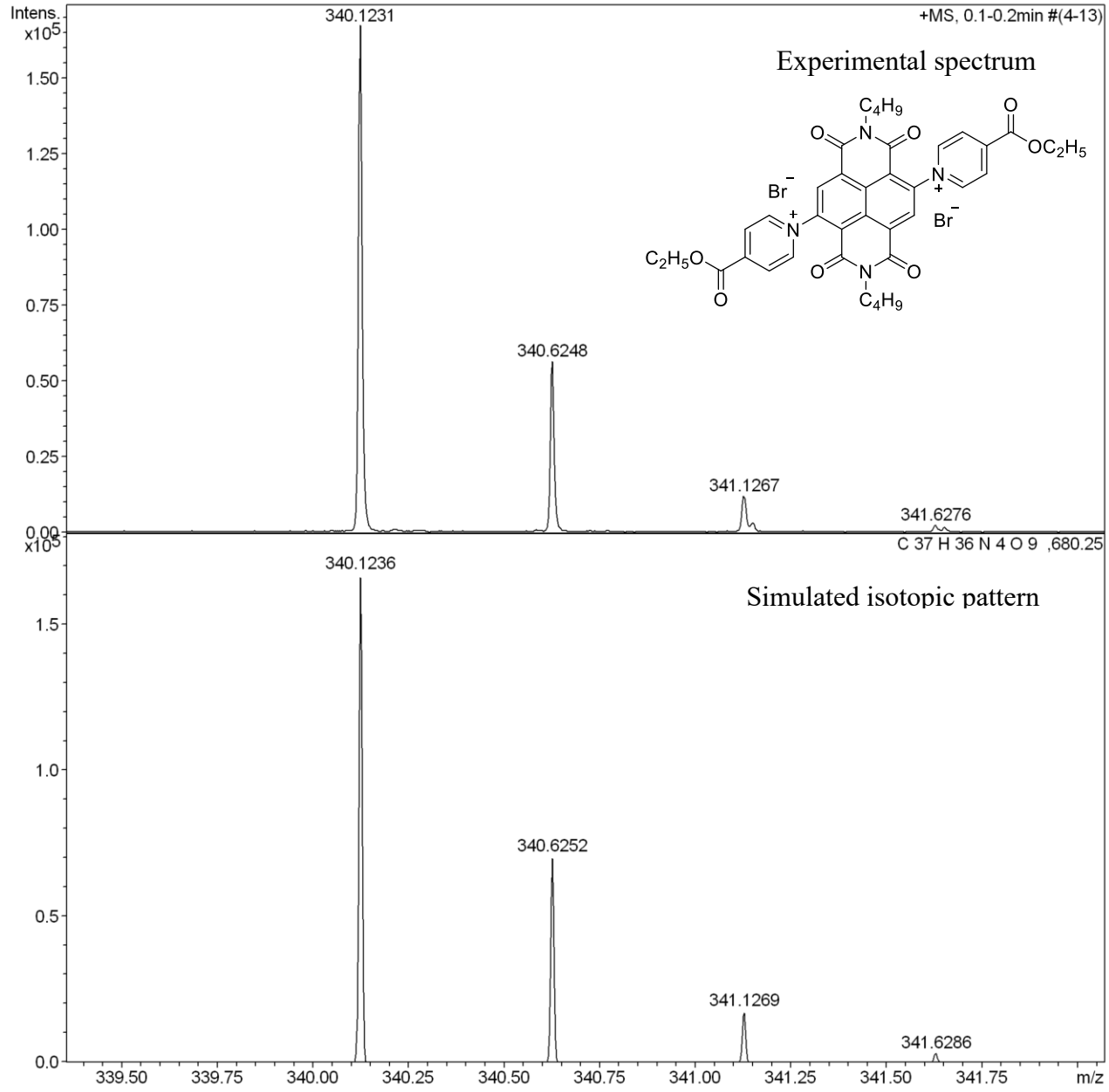

Figure S39. HRMS spectrum of **(C2^{2+})Br$_2$**.

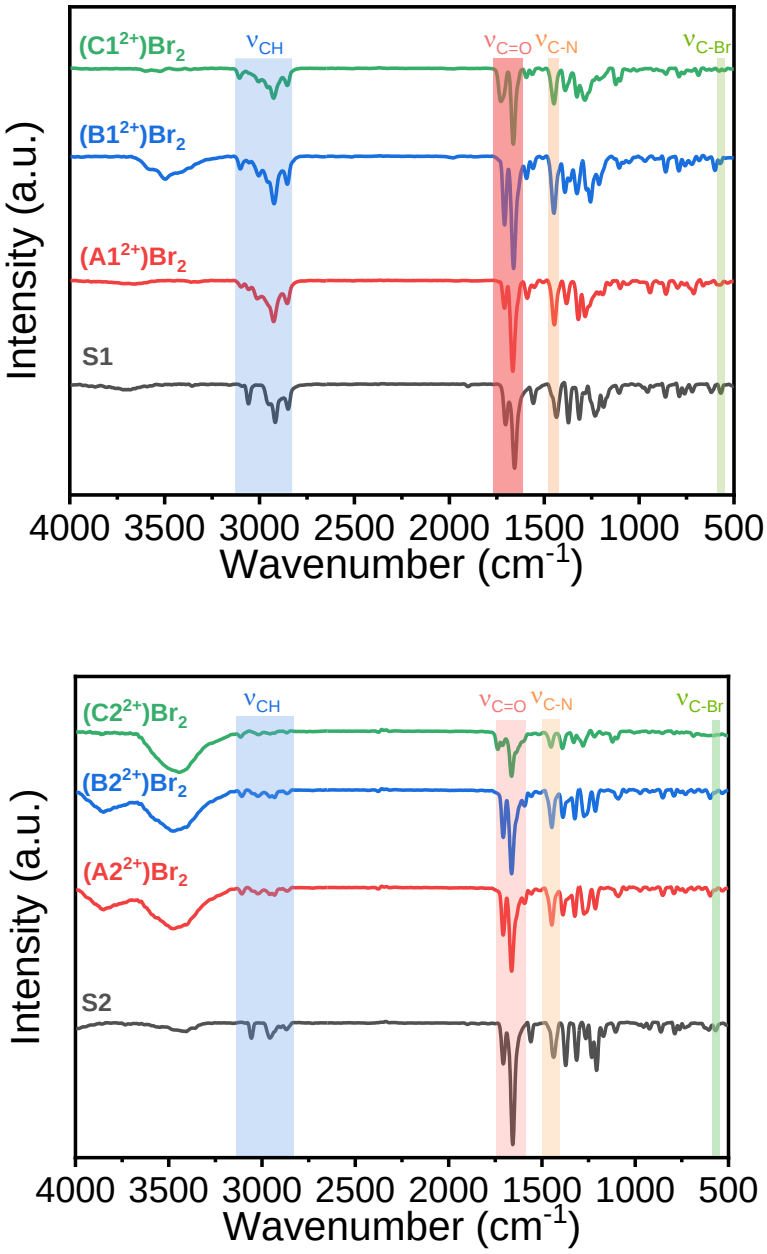

Figure S40. IR spectra of six NDI-carbonylpyridinium conjugates compared with their precursors **S1** and **S2**.

Table S1. Peak assignments in FTIR spectrum.

Samples	ν_{CH} (cm^{-1})	$\nu_{C=O}$(cm^{-1})	ν_{C-N} (cm^{-1})	ν_{C-Br} (cm^{-1})
S1	3059, 2918, 2849	1703, 1657	1435	569
$(A1^{2+})Br_2$	3096, 2926, 2855	1709, 1666	1447	-
$(B1^{2+})Br_2$	3101, 2924, 2855	1709, 1661	1448	-
$(C1^{2+})Br_2$	3105, 2926, 2855	1728, 1663	1448	
S2	3055, 2949, 2870	1705, 1655	1437	567
$(A2^{2+})Br_2$	3098, 2966, 2930	1709, 1666	1447	-
$(B2^{2+})Br_2$	3107, 3020, 2934	1707, 1663	1447	-
$(C2^{2+})Br_2$	3115, 3020, 2955	1738, 1663	1452	-

Compared to **S1** and **S2**, the aryl C-Br peaks at 567-569 cm^{-1} disappeared in NDI-carbonylpyridinium conjugates, manifesting the successful coupling reaction (also see Table S1).

References

[S1] (a) Sasikumar, M.; Suseela, Y. V.; Govindaraju, T. *Asian J. Org. Chem.* **2013**, *2*, 779-785. (b) Robitaille, A.; Jenekhe, S. A.; Leclerc, M. *Chem. Mater.* **2018**, *30*, 5353-5361.

[S2] Lai, W.-C.; Wang, S.-H.; Sun, H.-S.; Liao, C.-W.; Liu, T.-Y.; Lee, H.-T.; Yang, H.-R.; Wang, L.; Lai, Y.-Y. *ACS Appl. Polym. Mater.* **2022**, *4*, 521-526.

[S3] Lindström, H.; Södergren, S.; Solbrand, A.; Rensmo, H.; Hjelm, J.; Hagfeldt, A.; Lindquist, S.-E. *J. Phys. Chem. B* **1997**, *101*, 7717.

[S4] Liu, T. C.; Pell, W. G.; Conway, B. E.; Roberson, S. L. *J. Electrochem. Soc.* **1998**, *145*, 1882.

[S5] (a) Cui, Y.; Zhao, X.; Guo, R. *Electrochim. Acta* **2010**, *55*, 922-926. (b) Wang, S.; Wang, Q.; Shao, P.; Han, Y.; Gao, X.; Ma, L.; Yuan, S.; Ma, X.; Zhou, J.; Feng, X.; Wang, B. *J. Am. Chem. Soc.* **2017**, *139*, 4258-4261.